



FUAM

Journal of Pure and Applied Science

Available online at
www.fuamjpas.org.ng



An official Publication of
College of Science
Joseph Sarwuan Tarka University,
Makurdi.



Comparative Review of Conventional Computed Tomography and Photon Counting Detector Based Computed Tomography Systems

J. T^{1*} Iortile, L². Alumuku and I. D³ Shagu

¹Department of Radiology, Benue State University Teaching Hospital Makurdi, Nigeria

²Department of Pure and Applied Physics, Federal University Wukari, Wukari, Nigeria

³Department of Works and Maintenance, Benue State University Teaching Hospital Makurdi, Nigeria

*Correspondence E-mail: iortileter@gmail.com

Received: 17/02/2025 Accepted: 03/05/2025 Published online: 04/05/2025

Abstract

Computed Tomography (CT) has undergone significant transformations since its inception, with recent advancements in detector technology revolutionizing the field. This review provides an in-depth examination of conventional CT systems and the emerging photon counting detector (PCD)-based systems. Conventional CT systems, equipped with energy-integrating detectors, have been the cornerstone of medical imaging for decades. However, they are limited by their detector technology, resulting in compromised image quality, higher radiation doses, and limited spectral information. In contrast, PCD-based CT systems have broken new ground by offering improved imaging capabilities, including higher spatial resolution, increased sensitivity, and enhanced spectral distinction. The potential advantages of PCD-based CT systems are multifaceted, including reduced radiation exposure, improved diagnostic accuracy, and enhanced patient safety. This review provides a comprehensive analysis and performance characteristics of conventional CT and PCD-based CT systems, highlighting their clinical implications and applications, with a focus on their potential to transform various clinical specialties, including oncology, cardiology, and neurology. The review concludes by discussing the future direction of CT technology, including the potential for PCD-based systems to become the new standard in medical imaging. This review aims to educate and inform researchers, clinicians, and industry professionals about the latest developments in CT technology and their significant clinical impact. The proposed framework will enable improved and highly effective approach for brain, body, pelvic and cardiovascular diagnostics.

Keywords: Photon Counting, Image Reconstruction, Computed Tomography, Dose, Scanning Parameters

Introduction

Computed tomography was initially developed in 1972 and was later made commercially available for clinical use in 1974. Medical CT was first developed by British engineer Godfrey Hounsfield of Electric and Musical Industries (EMI), and American physicist Allan Cormack of Tufts University, Massachusetts [1]. The first clinical scanners which were dedicated to head imaging only were installed between 1974 and 1976. However, whole body systems became available in 1976 and in the 1980s it became widely available. The use of CT in medical practice in Nigeria dates back to more than 3 decades and ever since it has been experiencing increase in application and utilization [2]. Computed tomography uses a computer to process information collected from the passage of X-ray beams through an area of anatomy. However, as radiation-related diagnosis and treatment techniques become more sophisticated, a patient is more likely to be subject to radiation exposure that is too risky to ignore. While not overriding the benefits gained from the procedures, it is highly desirable to develop techniques to reduce patient dose without impacting the quality of care. One of the most diagnostic tools that can cause high

radiation doses is computed tomography (CT). According to the United Nations Scientific Committee on the Effects of Atomic Radiation (UNSCEAR), worldwide, CT constitutes approximately 6% of all medical X-ray examinations [3-5]. Due to increase of CT units being in use and added applications, the CT involvement to collective dose is growing during this decade.

The clinical uses of first- and second-generation CT scanners were limited largely to head scan protocols due to the long image acquisition times. Although improvements were made in the second-generation systems, few body scans were performed due to the long scan times and patient motion [6]. The limitations of the first- and second-generation scanners were eventually resolved with the improved features of a more updated CT system in the early 1980's. The "third-generation" CT scanners enhanced patient imaging by further reducing scan times and all together eliminating the translational motion of the previous systems. Third-generation CT scanners did this by employing the use of a full fan beam geometry which covered the entire FOV of the patient, meaning no translation motion was required. In this design, the X-ray



detectors were placed in an arc opposite the X-ray source, and the entire frame rotated around the patient as fast as possible [7-12]. The number of detectors in the third-generation CT scanners ranged from 256 to over 1000 detector elements. The increase in the number of detectors and full fan beam geometry reduced scan times to less than one second. The features of third-generation CT scanners not only improved patient scan times and image quality, but established the design for most of the modern CT systems we see today [6]. There has been a continuous technology in the improvement of CT generations up to 64 slices and above for imaging procedures across the hospitals.

Dose is another important issue in CT imaging and in many cases, the absorbed dose depends more on the imaging protocol as opposed to the scanning mode [13]. The absorbed dose in a CT scan is dependent on the pitch. The pitch is a parameter in helical scan modes which is defined as the table movement per 360-degree gantry rotation divided by the collimator width. Pitch is a fundamental parameter in helical imaging and it plays an important role in the absorbed dose, image quality, and scan time. For single detector array scanners, a pitch of 1.0 implies that the number of CT views acquired, when averaged over the long axis of the patient, is comparable to the number acquired with contiguous axial CT. A pitch of less than 1.0 involves over-scanning, which may result in a slight improvement in image quality but contributes a higher radiation dose to the patient [6]. Whereas, a pitch greater than 1.0 represents under-scanning and some of the transmission data measurements need to be interpolated [13].

The basic elements of the CT scanner are the X-ray tube, the detector or detector array, the image processing system and the image display system. The X-ray tube rotates around the patient while emitting a tightly collimated X-ray radiation photon beam. The beam is attenuated by the patient and strikes the detectors, which convert the photon intensity into a digital signal. Multiple profiles of patient attenuation are collected along lines or paths of known locations and integrated by the processing system [14-22]. An image is created from the attenuation data through a reconstruction algorithm. The algorithms developed for CT image reconstruction are many, but can be divided into iterative and analytic methods [23]. The changes in the fundamental structure of CT tubes and detectors are denoted as generations [24].

Generations of Computed Tomography Scanners

First-Generation Scanner

The first CT scanner was developed in the early 1970s by Hounsfield, a computer engineers in England [25]. The first generation of CT scanners utilizes a pencil beam X-ray source position at a fixed source interval with only one detector acquired image data by a 'translate-rotate' method. The combination of the X-ray tube and detector moved in a linear motion across the patient (translate) and this system motion was repeated until the beam and detector reached 180 degrees. When the X-rays were emitted from the source and penetrated through the patients, the intensity of X-rays was evaluated from a sequence of transmission

measurements made by the detector. This process is repeated for an acquisition of 180 projections at one-degree interval surrounding the patient generating 28,800 X-ray of total measurements. From these measurements an image was created. The first-generation CT scanners projected a succession of parallel beams at different locations through the patient as it does translate linearly across a specific field of view (FOV). When the system has completed the appropriate field of view for a particular examination, it rotates one degree and the translation process is repeated in the following projection [6]. One advantage of the first-generation CT scanner was that it employed pencil beam geometry-only, two detectors measured the transmission of X-rays through the patient. The pencil beam allowed very efficient scatter reduction, because scatter that was deflected away from the pencil ray was not measured by a detector. With regard to scatter rejection, the pencil beam geometry used in first-generation CT scanners was the best [6]. However, the disadvantage of these scanners was the scan time, which took approximately 4 - 5.5 minutes to produce an image, and the limitation of the device to the head only [9]. Figure 1 below shows the first-generation CT scanner, which used a parallel X-ray beam with translate-rotate motion to acquire data.

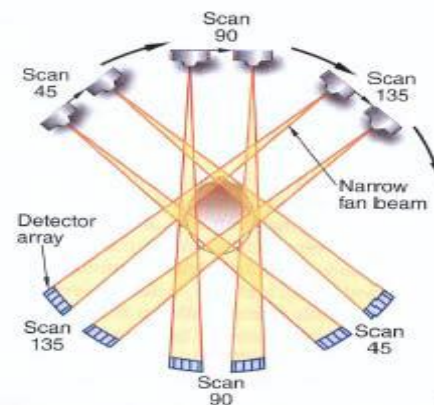


Fig. 1: The First-Generation Scanner

From Carlton/Adler. *Radiographic Imaging Concepts and Principles*. International Edition, 5E © 2013 Delmar Learning, a part of Cengage Learning, Inc. Reproduced by permission.

www.cengage.com/permissions

Second-Generation Scanner

The second generation of CT was introduced in 1972 for the purpose of improving image quality and scan time. The X-ray source was changed from the pencil beam to a narrow fan shaped beam geometry (10 to 15 degrees) together with multiple detectors. These scanners decreased the scan time and improved the image quality, but increased the amount of scatter radiation [26]. With improvement made from first to second generation CT scanners, the average scan time was reduced from few minutes to few tens of seconds. The angle of rotation between the translation motions increased considerably as a result of the narrow fan beam and multiple arrays of detector system used. Data analysis and processing efficiency was improved



per rotation through the multi detector system, minimizing the total number of revolutions required to produce an image and the increase in detector number from 2 to 30 improve the X-ray beam use to produce the image. The clinical use of the first and the second-generation CT scanners were only restricted to head scan protocols due to prolong image acquisition time. However, with the improvement made on the second-generation CT scanners, a few body scans were executed. Figure 2 below shows the second-generation CT scanner, which used translate-rotate motion to acquire data.

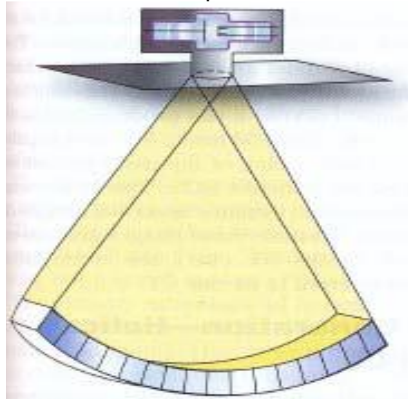


Fig. 2: The Second-Generation Scanner

From Carlton/Adler. *Radiographic Imaging Concepts and Principles. International Edition*, 5E © 2013 Delmar Learning, a part of Cengage Learning, Inc. Reproduced by permission.
www.cengage.com/permissions

Third-Generation Computed Tomography Scanners

The number of detectors used in third-generation scanners was increased substantially, and the angle of the fan beam was also increased so that, the detector array formed an arc wide enough to allow the X-ray beam to interact with the entire patient. Third generation CT scanners saw the evolution of elements of the modern CT scan, which uses a wide fan shaped beam and a curved detector array with up to 750 detectors. The wide fan beam was wide enough to include the whole patient in an individual exposure. These scanners decreased the scan-time to nearly one seconds for a single image and improved the image quality, but the use of a moving detector created a problem called a 'ring artifact' [26]. Figure 3 below shows the third-generation CT scanner, which acquires data by rotating both the X-ray source with wide fan beam geometry and the detectors around the patient.

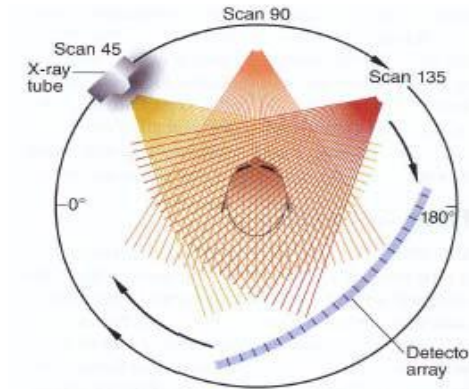


Fig. 3: The Third-Generation Scanner

From Carlton/Adler. *Radiographic Imaging Concepts and Principles. International Edition*, 5E © 2013 Delmar Learning, a part of Cengage Learning, Inc. Reproduced by permission.
www.cengage.com/permissions

Fourth-Generation Scanners

Fourth-generation CT scanners were designed to overcome the problem of ring artifacts. With these CT scanners, the detectors are removed from the rotating gantry and are placed in a stationary 360-degree ring around the patient, requiring many more detectors. Modern fourth-generation CT systems use about 4,800 individual detectors. Because the X-ray tube rotates and the detectors are stationary, fourth-generation CT is said to use a rotate/stationary geometry. The design was based on a rotating X-ray source and stationary detector and achieved scan-time ranges from 2 to 10 seconds [26]. Figure 4 below shows the fourth-generation CT scanner, which uses a stationary ring of detectors positioned around the patient.

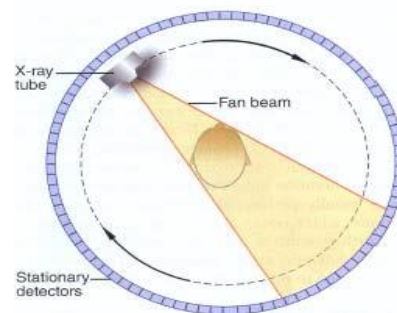


Fig. 4: The Fourth-Generation Scanner

From Carlton/Adler. *Radiographic Imaging Concepts and Principles. International Edition*, 5E © 2013 Delmar Learning, a part of Cengage Learning, Inc. Reproduced by permission.
www.cengage.com/permissions

Fifth-Generation Scanners



This generation of scanners is referred as cardiac cine CT or Electronic Beam Tomography (EBT). The parts in these systems are stationary for which; the X-ray source and detectors are both fixed. These groups of scanners do not look like that of the conventional X-ray tube, but consist of a large semi-circle ring that surrounds the patient, allowing high speed CT scanning to acquire up to 17 images per second [26]. Figure 5 below shows the fifth-generation scanner for which the X-ray source and detectors are both fixed.

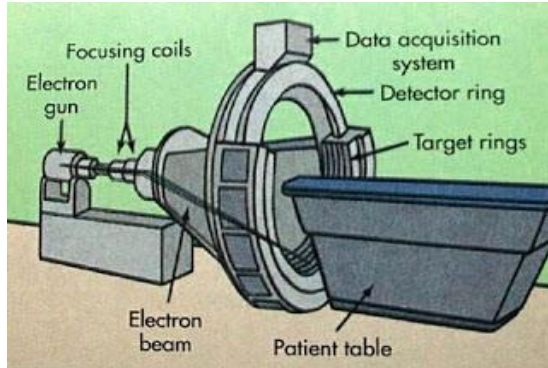


Fig. 5: The Fifth-Generation Scanner

Source: www.computedtomographyct.blogspot.com (Accessed November, 2024)

Sixth Generation (Helical)

These generations of scanners are also Helical/Spiral CT, which uses slip ring technology, where many images are acquired while the patient is moved through the gantry [27]. Normally in helical CT, the X-ray tube is continuously rotating while the table (couch) is fixed during the examination; allowing patient images to be acquired within one single breath hold [9]. The design of slip ring technology comprises of many sets of matching rings to allow the current and voltage to the X-ray tube, without cables connecting directly to the tube. This avoids the X-ray tube from stopping during its continuous rotation. The main advantages of these scanners include the shorter scan time, avoiding overlap and reduction in the motion 'artifact' [26]. Figure 6 below shows the sixth-generation scanner for which the X-ray tube is continuously rotating while the table (couch) is fixed during the examination.

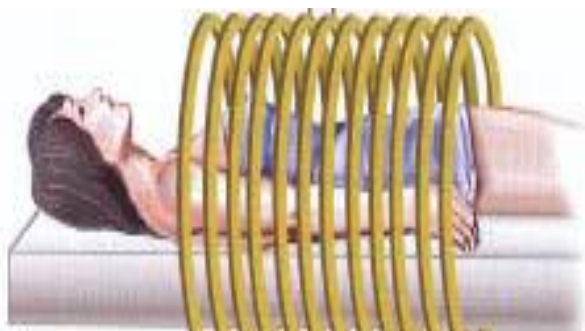


Fig. 6: The Sixth-Generation Scanner (Helical)

From Carlton/Adler. *Radiographic Imaging Concepts and Principles. International Edition*, 5E © 2013 Delmar Learning, a part of Cengage Learning, Inc. Reproduced by permission. www.cengage.com/permissions

i. Modern Computed Tomography Scanners

Modern-day CT scanners fall into two categories: (1) scanners defined by the helical or spiral single-detector mechanism and (2) increased density of multi-slice detectors

ii. Multi-slice Computed Tomography Scanners

Multi-slice CT scanners include more than one ring of detectors. The number of slices has increased with time, with up to 320 slices per revolution currently being offered. This structure employs a 'step and shoot' approach to data acquisition. With a thick enough ring of detectors, it is possible to cover the entire heart within a single revolution. With greater than 16 slices per revolution, the X-ray tube no longer produces a beam, but rather a cone [21]. The need for faster CT scan times led to the development of scanners using spiral helical geometry (also known as continuous rotation scanners, or volume scanners). The process differs from multi-slice image acquisition in that data are collected in volumes rather than individual slices. This geometry relies on slip-ring technology, which allows continuous rotation of the gantry. The terms 'spiral geometry' (Siemens) and 'helical geometry' (Toshiba) describe the path traced by the X-ray tube, or fan beam, during the scanning process [21]. The single-slice CT has the advantage that a patient can hold their breath for the duration of the whole CT scan, which minimizes patient movement [6]. The multi-slice CT was introduced in 1991 [28]. This scanner is capable of producing more than one image per tube rotation. The difference between the MSCT and the SSCT is that it has multiple rows of detectors [29]. The latest MSCT is capable of producing up to 320 slices per tube rotation [21]. Figure 7 shows the scan pattern of multi-slice CT scanner with detector array configurations.

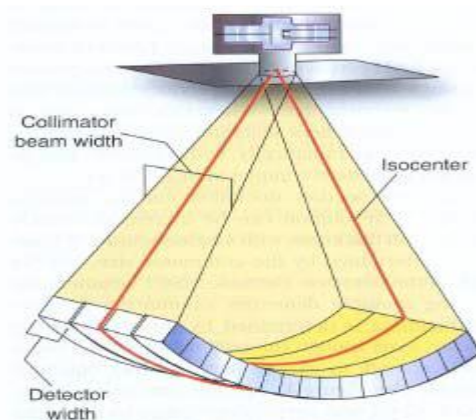


Fig. 7: Scan Pattern of Multi-slice CT Scanner



From Carlton/Adler. *Radiographic Imaging Concepts and Principles. International Edition*, 5E © 2013 Delmar Learning, a part of Cengage Learning, Inc. Reproduced by permission. www.cengage.com/permissions

iii. **The Dual Source Computed Tomography Scanner**

The quest for better spatial and temporal resolution has led to the development of the dual source CT scanner (DSCT). The DSCT relies on two X-ray tubes located at right angles from each other, coupled with their opposite detectors. As the detectors rotate together, a rotation of only 90 degrees is needed to collect the information for which a single-source scanner needed a 180-degree rotation to detect. This technological advancement provides the excellent temporal resolution needed to image the heart by reducing the effective gantry rotation time by 50 per cent [8].

iv. **Seventh Generation Scanners: Flat Panel Computed Tomography Scanners**

The current development of new CT technology looks to use the advances of digital radiography detector arrays to improve the spatial resolution of the CT image. Unlike the sixth generation of CT scanners—which take a continuous one-dimensional reading—the seventh generation relies on flat panel detectors, similar to those used in current digital radiography, to collect a series of two-dimensional images. The detector consists of an array of thin-film transistors mounted with a caesium iodide scintillator [21]. Due to its capacity to take large volumes of data at one time, it is also known as Volume CT [30]. Figure 8 below shows the prototype of the seventh generation CT scanner and its

components

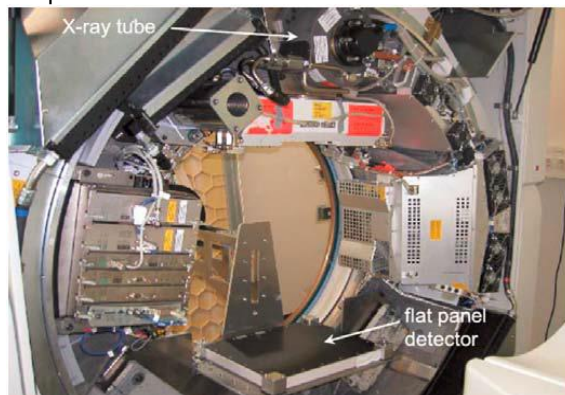


Fig. 8: Prototype of Seventh Generation CT Scanner

From Seeram. *Computed Tomography: Physical Principles, Clinical Applications, and Quality Control*. 3rd Ed. © 2009. Reproduced by permission from Saunders Elsevier

Components of Computed Tomography System

The configuration of components in CT systems varies depending on the generation and manufacturer. The basic

functions of machine components are similar. CT systems mainly comprise of two components, the computer system and the scanner

Computer

The computer performs a variety of tasks in the CT process. Use of computer systems has numerous advantages including substantial enhancement in the volume of images it can store and retrieve, highly accelerated speed and increased accuracy in data communication. The single function performed by the computer that distinguishes the CT image is the reconstruction process. The computer unit includes several hardware (mechanical) components that execute the specific software programs used to reconstruct and manipulate the imaging data. These units are all kept in the control room, where temperature and humidity are controlled to protect the integrity of the mechanisms. The five hardware elements include: [28].

- i. **System console (or input device):** The system console is the main control center from which the technologist gives instructions to the entire CT system. Most modern consoles have a look and feel similar to a personal computer (PC) (keyboard with mouse). Older units utilize plasma screen technology. Using these devices, the technologist is able to input scan parameters, patient information, and instructions for post processing, filming, archiving, and networking. The appearance of this screen is called the "user interface". Many systems utilize graphic images to initiate tasks, e.g., folders or icons. The combination of these icons and the workflow is referred to as the Graphical User Interface (GUI) [28].
- ii. **Central processing unit:** The central array processing unit or CPU (also referred to as the image reconstruction system (IRS), is where the raw data are received and reconstructed into the final CT image. The appearance of the final image is influenced by reconstruction algorithms. Modern CPU/IRS is asked to perform a huge number of image reconstruction calculations at blinding speeds. Post processing can be done at the scanner or at separate work stations depending on the type of license and type of equipment. Once processed, images are sent to an output device such as a laser printer, Picture Archival and Communication System (PACS), Digital Versatile Disk (DVD), Compact Disc Read-Only Memory (CD-ROM), external Universal Serial Bus (USB) drive or offline workstation [31].
- iii. **Internal memory (or hard drive):** Two types of internal memory are used in every CT computer system, each serving a different function. Read-only memory (ROM) is reserved for long-term storage of internal data, such as the operating system while Random-access memory (RAM) is available for the temporary storage of information, such as the data received from an individual CT scan. Internal memory on a computer is located on the hard drive and



retained on hard disks sealed within the hard drive. This type of memory is accessible to the user through the input devices [31].

- iv. **Output device:** These are devices that provide feedback to the user. This could be screens such as cathode ray tube or liquid crystal display television sets. Laser cameras can be employed to record CT images for interpretation. All systems now utilize a 14"x17" size film with image formatting varying between 12:1, 15:1, and 20:1 [28], [31].
- v. **External memory (or storage unit):** Older systems utilized a compact form of data storage called Magnetic Optical Discs (MOD) that held several gigabytes of data, allowing greater amounts of data to be archived in a small space. A busy CT practice could store a year's worth of cases on one or two bookshelves. Optical disks use a laser beam to write (burn) data as binary code into the surface of a metallic disk. Two types of disks are used: the write-once-read-many (WORM) disk with a storage capacity from 122 megabytes (MB) to 6.4 gigabytes (GB) and a rewritable/erasable disk with a capacity of 2.5 GB, which is used to accommodate the need for frequent updates of the data on a file. In recent years, the DVD has become a very good storage medium, holding up to 4.7 GB of data and physically much more compact than MODs. External hard drive devices are commonly used to archive data and are capable of holding mass amounts of data from gigabytes to terabytes. But by far the largest and most efficient form of data storage and display that involves networking data to large storage main frames is a Picture Archiving Communication System (PACS) with storage capacities of multiple terabytes (one billion bytes or 1000 gigabytes) [25]. Computed tomography tasks can be subdivided into three basic categories, each of which utilizes unique software: [25].
 - a. **Operating system of the computer:** This is the permanent software program through which all applications must run.
 - b. **Applications programs:** These are developed to execute specific tasks and are at the level at which instructions are input into the system to initiate all mechanical processes, as well as receive information and submit it to output and storage. The technologist needs to be thoroughly familiar with the use of the applications software in order to run the system [25].
 - c. **System tools.** These tools are the computer languages the system requires to execute the applications. They are also used by service technicians for system maintenance, upgrades, and problem solving [25].

Scanner components

The imaging system of the machine is made up of the following components:

1. **Scan Controller:** it receives instructions from the host computer and in turn regulate the operation and timing of the patient table, the gantry, and the high-voltage generator.
2. **Data Acquisition System (DAS):** this is a set of electronics located between the detector array and the host computer. It controls the operations of the system that influence the intake of data. The DAS amplifies the signal emanating from the detector, converts the signal to digital, and then sends it on to the computer. On a modern CT system, these functions must be completed for over 700 detectors each time the tube sweeps around the patient (usually in less than a second). The components of the DAS that perform these tasks include the digital-to-analog converter, high voltage generator, amplifier, sample/hold, and the analog to digital converter [28].
3. **Digital-to-Analog Converter (DAC):** before the instructions from the scan controllers (in the form of signals) can be interpreted, the signals must be converted into a continuous analog waveform signal. This conversion is performed by the DAC located between the scan controller and the gantry [28].
4. **High-Voltage Generator (HVG):** the high voltage generator is the unit that generates the voltage necessary to produce X-rays. Depending on the generation of the scanner, the HVG may be located either inside or outside the gantry [28].
5. **Transformer:** this is another form of high voltage generator. It provides the CT units with necessary voltage to operate. The voltage supplied from the mains is usually less than what the scanner needs to operate. The transformer is often a step-up transformer that amplifies the voltage, giving the tube the necessary power to operate [28].
6. **Amplifier:** this is where signals go immediately after leaving the gantry. These analog signals are amplified without conversion and sent to the sample/hold unit [31].
7. **Sample/Hold (S/H):** this is located between the amplifier and the analog-to-digital converter (ADC). This is where the area/region of interest is sampled to differentiate among structures with various densities and then assigned various shades of gray to the pixels to represent those structures. The S/H determines the relative attenuation of the beam by the tissues that were scanned [31].
8. **Analog-to-Digital Converter (ADC):** the ADC is the unit that takes the analog signal output by the scanning equipment and converts it into a digital signal that can be understood and analyzed by the computer. The unit has three major components to perform three separate operations: sampling, quantization, and coding. In sampling, the system takes portions, or samples, of the continuous analog signal. The quantizing component processes the sample data into discrete-time, discrete-value signals. Next, the digital signal is coded with a specific binary bit sequence



correlating to each sample of output from the quantized [31].

9. **Array Processor:** the array processor is a specialized high-speed computer that takes hundreds of detector measurements from hundreds of different projections and pieces them back together at a very high rate. The array processor is also responsible for retrospective reconstruction and post processing of image data. The number of array processors affects the image reconstruction time, which is the time it takes to reconstruct the images in the dataset [31].
10. **Gantry:** All of the components for generating X-rays, moving the tube around the patient, collimating to the appropriate protocol-driven slice thickness, and the detectors are contained in a unit called the gantry. The gantry is designed with a round aperture of about 50–85 cm to allow room for insertion of both the patient and the table. The X-ray tube and detectors are located at the interior aspect of the gantry assembly, which is the portion of the mechanism that rotates around the patient. Depending on the region of interest, the gantry may need to be tilted. Some models of gantries may be designed to tilt to up to a $\pm 30^\circ$ angle to adjust positioning. Gantry tilt is severely limited with some types of multi-slice CT systems. Depending on the geometry and the algorithm processes of the multi-slice detector, gantry tilt may or may not be available. Today there are systems that utilize an adjustable head holder, tilting various degrees to compensate for gantry angulations. It is important that the patient be positioned so that the region of interest is centered within the scan field and well away from the outer edges of the scanning field where the image quality is poor. Positioning lights mounted to the gantry are arranged in sets of three to help the technologist align the patient properly [31].

11. **Patient Table or Couch:** The patient lies on the table (or couch, as it is referred to by some manufacturers) and is moved within the gantry for scanning. The process of moving the table by a specified measure is most commonly called incrementation, but is also referred to as feed, step, or index. Helical CT table incrementation is quantified in millimeters per second because the table continues to move throughout the scan. The degree to which a table can move horizontally is called the scan able range, and will determine the extent a patient can be scanned without repositioning. A numeric readout of the table location relative to the gantry is displayed. When the patient is placed within the gantry, an anatomic landmark, such as the xiphoid or the iliac crest, is adjusted so that it lies at the scan point. At this level, the table is referenced, which means that the table position is manually set at zero by the technologist. Accurate table referencing helps to maintain consistency between examinations. For example, if a lesion is seen on an image that is 50 mm inferior* to the xiphoid landmark (zero point), the patient is removed from the gantry, and a ruler is used to measure 50 mm inferior from the xiphoid. This point provides an approximation of the location of the lesion. This system is also helpful if the scan will be repeated at a later date, exclusively through the area of interest determined on the earlier scan. For this reason, the setting of landmarks must be consistent among CT staff. The

specifications of tables vary, but all have certain weight restrictions. If the patient's weight exceeds the specified limits, scanning is often still possible. However, the table increments may not be as accurate. This problem affects small table increments more than those 5 mm or larger. On most scanners, it is possible to place the patient either head first or feet first, supine or prone. Patient position within the gantry depends on the examination being performed. Various attachments are available for specific types of scanning procedures. For example, attachments for direct coronal scanning of the head and for therapy planning are common. Each table has a maximum weight recommendation of 400 (180) to 485 (220) lbs (kgs); bariatric tables can hold up to 660 lbs (300 kg), depending on the size of the gantry aperture [31], [32].

Computed Tomography Scanner Design

Scanner design features affect radiation dose to the patient. Most of the features of CT scanners that affect dose and dose efficiency are similar in both single and multi-slice systems. Features of CT scanners that affect patient's dose include: tube filtration, beam shaping filters, collimator design, and focus to axis distance. Those that affect dose efficiency include: detector materials, number, width and spacing. Indeed, some manufacturers have a range of systems from single to 16-slice which are identical in terms of most of the features. The only difference is that the single bank of detectors of a single slice scanner is replaced by multiple detector banks along the z-axis. It is this factor which primarily causes differences in dose efficiency between single and multi slice scanners [15], [33]. Also, the difference in number of detector rows affects the DLP due to an increase in area coverage but not the $CTDI_{vol}$ if parameters like kVp and mAs are kept constant [15].

Operating Parameters for Computer Tomography Scan

Various changes in selectable scan operating parameters affect patients' radiation dose. These include: changes in source collimation, section thickness, section spacing, and number of adjacent sections. Some scanners have a much wider choice of operating parameters than others [34]. Previous studies have suggested that it is feasible to reduce tube current without marked deterioration of image quality in CT of the head [35]. Other operating parameters that significantly affect radiation dose to patients are:

X-ray tube voltage: is the electrical potential applied across the X-ray tube to accelerate electrons toward the target material. Radiation dose increases approximately proportional to the percentage change in tube voltage [36].

X-ray tube current: increasing the current (mA) increases the dose proportionately [37].

Scan time: in a complete rotation of 360° , dose is directly proportional to scan time. If incomplete rotations are employed, there is a complex spatial relationship between dose and scan time because of variations in rotation angle. The exposure time may be significantly less than the set scan



time for scanners that employ a pulsed X-ray beam. Therefore, a longer scan time leads to more radiation dose to patients [34]. Thin slice sections give more doses to patient because the CT scanner will take more time to cover the desired area of interest [9].

Scanner rotation angle: The desirable reconstruction angle for CT image is 180° . Data acquisition over 360° (or 360° plus over scan) is widely used for third and fourth generation scanners. Over scan is often used to reduce patient motion artifacts. Some scanners may irradiate patients over a larger angle than that used for data collection as the tube accelerates and decelerates before and after the scan. Any rotation other than 360° will result in an asymmetric dose distribution. This is most marked for 180° scans, which may be employed when scanners operate in the fast-scanning modes such as that used for dynamic studies [34]. A rotation angle of 360° produces more radiation dose [38]. Equally, additional rotation generally contributes a greater percentage to the radiation dose more especially in a multi-slice CT scanner [39].

Filtration: This is the scanner component that shapes the energy of the X-ray spectrum. Beam shaping is done using either a bow tie filter and/or flat filters. The radiation output from the X-ray tube (CTDI_w) is affected by a change in beam shaping filters. The relationship is vendor and filters specific [36].

Patient orientation: patient orientation (supine or prone positions) may significantly affect the dose to critical organs such as the eyes when acquiring the scanogram [37]. The chance of the effect becomes higher when the x-ray tube is at the fronto-occipital position. This is because the critical organ (the eye) is closer to the source of radiation. Unfortunately, this is of less importance in brain CT scan, because in modern CT scanners the orientation of the x-ray tube could be changed from fronto-occipital to occipito-frontal position. In addition, the gantry could be angled to minimize dose to the lens of the eyes without changing the patient position.

Source collimation: X-ray beam collimation defines the beam width for examination. Wider beam collimation however, more penumbra which does not contribute in image formation but rather affect the radiation dose [21].

Section thickness: Increasing the slice thickness yields a slightly lower dose per scan as well as decreased noise. Decreasing the section thickness while keeping noise constant results in higher radiation doses [33-34].

Section spacing: Decreasing section spacing increases multiple-scan dose [34].

Pitch: It is defined based on the International Electro technical Commission standards, as the table travel divided by the total active detector length in the Z-axis (GE Medical System, 2001). Most manufacturers give pitch value with respect to the nominal slice thickness instead of the total active collimated length in the Z-direction. This definition of

pitch is easier to use in both single and multi-slice systems. In helical CT, selecting a higher pitch will reduce the DLP of the patient but not the CTDI, by reducing the number of rotations over the same plane (GE Medical [21], [40].

Number of adjacent sections: Increasing the number of adjacent sections increases the volume of tissue irradiated, and increases the dose to any individual region of the patient when the dose profiles overlap [21].

Repeat scans: Repeat scans of the same region increase radiation dose to patient [21].

Image parameters: selectable image parameters such as pixel size and reconstruction filter do not affect dose directly. The dose however, varies when a change in these parameters requires a different scan time to obtain the desired image quality [34], [37].

Standard scan examination: outline of scanning procedure for a particular clinical indication that is generally accepted as being able to provide adequate clinical information in most of the patients examined. Radiation doses are usually lower than that of special techniques [38]. In a study conducted by [41], they stated that dose reduction from 0.9 mSv to 0.7 mSv without significant change to image quality is possible if the scan is done with standard exposure factors such as 120 kV, 250 mAs, 5 mm nominal slice thickness and with distal slice increment less than one instead of scanning with 120 kV, 250 mAs, 0.5 mm or 1mm slice thickness with slice increment greater than one.

The patient: dose distribution depends on the size, shape, tissue density, and elemental composition of the patient cross section. The same scanner types with the same operating technique would have different dose distributions for different body parts. A thicker patient section or denser tissue results in more attenuation of the primary beam and more build-up of scattered radiation. The dose at any point in the section is the sum of contributions from many beams, which may have undergone different amounts of attenuation [34]. To establish DRLs for different body parts, [42], recommended that measurements be performed on standard-sized patients or patients close to standard size, preferably with an average weight, that is 70 kg.

Computed Tomography Imaging

There are two steps necessary to obtaining a CT image. Firstly, physical measurements of the attenuation of X-rays traversing the patient in different directions and secondly mathematical calculations of the linear attenuation coefficients, μ , all over the slice. The procedure is as follows: The patient remains stationary on the examination table while the X-ray tube rotates in a circular orbit around the patient in a plane perpendicular to the length-axis of the patient. A fan-shaped beam of variable thickness (1-10 mm), wide enough to pass on both sides of the patient is used. The X-ray tube is similar to but more powerful than those used in planar radiography. The image receptor is an array of several hundred small separate receptors. Readings from



the receptors are fed into a computer which, after numerous calculations, produces a tomogram of the patient, i.e., a map of linear attenuation coefficients μ . The receptors measure the X-rays coming through a slice of the patient in different positions forming one projection of the patient. The reading in any one receptor is a measure of the attenuation in the patient along the path of a particular ray. Behind a homogeneous object, the receptor reading is given by:

$$I = I_o e^{-\mu t} \quad (1)$$

Where I_o is the receptor reading without the object and μ the linear attenuation coefficient for the object, t is the object thickness along the path of that ray and e the base of the natural logarithm ($e = 2.718$). For an inhomogeneous object such as a patient, the product μx is a sum over all the different tissue types, i , $\sum \mu_i x_i$. Given data from sets of projection profiles through all volume elements (voxels) in a slice of the patient for sufficient numbers of rotation angles (projections), it is possible to calculate the average linear attenuation coefficient, m , for each voxel. This procedure is called reconstruction. Each value of μ is assigned a grey scale value on the display-monitor and is presented in a square picture element (pixel) of the image.

Reconstruction algorithms

The computer reconstructs an image, a matrix of μ -values for all voxels in a slice perpendicular to the rotation axis. The procedure to reconstruct the image, based on the many projections at different angles, is made with a reconstruction algorithm. An algorithm is a mathematical method for solving a specific problem. The problem here is to find the μ -values in each voxel based on all the measured data in the projection profiles. The mathematical problem of two-dimensional image reconstruction is solved using integrals, a method developed by Radon in 1971 [9]. Consider an X-ray beam with initial photon intensity I_o traveling through an object described by the linear attenuation coefficient $f(x, y)$. After travelling through the object, the remaining photon intensity $I(r, \theta)$ is given by: [9]

$I(r, \theta) = I_o \exp - \iint f(x, y) ds$ (2) Taking the logarithm yields,

$$p(r, \theta) = -\ln \left(\frac{I(r, \theta)}{I_o} \right) = \iint f(x, y) ds \quad (3)$$

This is the total attenuation of a ray on a position r , on the projection at an angle θ . Using the coordinate system in the equation below; the value r onto which the point (x, y) will be projected at angle θ is given by: [9]

$$x \cos \theta + y \sin \theta = r \quad (4)$$

Several types of reconstruction algorithms are available including filtered back-projection, direct Fourier and algebraic reconstruction techniques. The method used for medical CT scanners is filtered back-projection. In filtered

back projection, digital image processing algorithms that are used to improve image quality or change certain image quality characteristics, such as detail and noise. The corrected attenuation of rays obtained from ray paths are then sent back along the paths and used to obtain images [9].

Display of Computed Tomography Numbers (N_{CT})

In the display the measured μ -values can be distributed over a grey scale with the lowest values of μ black and the highest white. Different substances such as gas (air), fat, soft tissues (including blood, muscle, liver, brain and cartilage) and bone are distinguishable in the image. In CT imaging, these substances are assigned different values for display. Most soft tissues have linear attenuation coefficients very similar to that of water over a large photon energy interval. This is the reason for defining a CT number, CT_{number} as: [9]

$$CT_{\text{number}} = \frac{\mu - \mu_w}{\mu_w} \times 1000 \quad (5)$$

Where μ is the average linear attenuation coefficient for the material in a given voxel and μ_w that for water. CT_{number} is given in the dimensionless unit Hounsfield, H. The CT number scale has two fixed values independent of photon energy. For vacuum (air or body gas) $CT_{\text{number vac}} = -1000$ and for water $CT_{\text{number w}} = 0$ [9].

Alternatively, the μ -values may be graphically displayed. Normalization with μ_w in the equation above diminishes the variation of CT_{number} with energy especially for materials with atomic numbers similar to that of water. All the soft tissues mentioned in connection with the X-ray elements fulfill this condition. This is why, CT_{number} for these tissues may be the same for all users over a broad energy interval (40-150 keV) including the spectra used in clinical CT scanners. CT_{number} for fat and especially for bone vary however in different applications. Any material that possesses absorption properties that are higher than water takes a positive value. Similarly, any material that has absorption properties that are lower than water takes a negative value [9].

Computed Tomography Artifacts

Computed tomography artifacts are errors in the perception or representation of visual or aural information introduced by the involved equipment or techniques. The major artifacts of a computed tomography (CT) are:

Ring artifacts

This occurs as a result of one or more malfunctioning detectors, and unusable images, which may result from malfunctioning of the X-ray tube during the acquisition. Under sampling the projection data may lead to Moiré patterns, and detector afterglow may induce blurring of the image [9].

Partial volume or volume averaging artifacts

It occurs when thick acquisition slices are used which results from an averaging of the linear attenuation coefficient along the z axis of a voxel. It will make a small high-density object



appear as a larger lower density object and is seen, for example, when looking at cortical bone in thick CT slices. This can be avoided by the use of thinner slices [9].

Motion artifacts

These often appear in scans of the abdomen due to movement of gas bubbles in the intestines. If an in pocket moves during the scan, inconsistent data is presented to the computer, which then has trouble reconstructing a proper image. The image usually includes extraneous black lines emanating from the region of the gas bubble. These artifacts may at times interfere with a diagnosis. Artifacts of this kind are minimized in the type one and fourth generation scanners, which perform scans in 2-3 seconds [9].

Beam hardening artifacts

Occurs as a result of strong attenuation of the X-ray beam by compact bone, calcifications or a metal object [9].

Aliasing

These occurs when a sharp and high contrast boundary (as at a bone edge) may produce a number of parallel streaks nearby in the image as observed in the boundary between the lung and diaphragm leading to spurious increase in density appearing in the base of the lung [9].

Image Noise in Computed Tomography Systems

Image noise is the fluctuation in the input signal being processed. Several sources might be contributory to the variations and could be in form of additions or subtractions that alter the true form of the signal. Some of these sources that produce image noise are discussed below [9].

Random noise

This is a combination of various fluctuations in the image density that change from one image to the next in an unpredictable and random manner. This type of noise is present in radiographs taken with fast screen-film combinations in form of radiographic mottle [43].

Statistical noise

The energy in X-ray beams is transmitted in the form of individual chunks of energy called quanta. Hence the response of an X-ray detector is actually the result of detecting a finite number of X-ray quanta. The number of detected quanta will vary from one measurement to the next, not because of inadequacies in the detection apparatus, but because of statistical fluctuations that naturally arise in the "counting" process. As more quanta are detected in each measurement, the relative accuracy of each measurement improves. Statistical noise in X-ray images arises from the fluctuations inherent in the detection of a finite number of X-ray quanta. Statistical noise may also be called quantum noise and is often referred to as quantum mottle in film radiography [6]. If N is the number of photons measured per unit area by a detector, then the noise of a digital X-ray detector system with square pixels is

$$\sigma = \sqrt{N} \quad (6)$$

Where σ is the standard deviation or noise [6]

Statistical noise clearly represents a fundamental limitation in X-ray radiographic processes. The only way to reduce the effects of statistical noise is to increase the number of detected X-ray quanta. Normally this is achieved by increasing the number of transmitted X-rays through an increase in dose [6].

Electronic noise

In processing electric signals, electronic circuits inevitably add some noise to the signals. Analog circuits, those which process continuously varying signals, are most susceptible to additional noise. The difficulty of noise suppression is compounded by the fact that for some types of X-ray detectors, the electronic signals are very small. There is evidence [44] that many commercially available CT scanners are sufficiently well engineered to reduce the contribution of electronic noise under normal operating conditions to a fraction of the statistical noise contribution. The signals are converted to digital or discrete form in the signal-processing step and then sent to a computer for reconstruction.

Round-off errors

This type of noise is common to digital computers. Although digital computers are not subject to electronic noise, they do introduce noise in the reconstruction process through round off errors. The errors arise from the limited number of bits used to represent numbers in the computer. For example, the product of two numbers must be rounded off to the least significant bit used in the computer's representation of the number. Round off errors can normally be kept at an insignificant level either through choice of a computer with enough bits per word or through proper programming [6]. Round off errors can and do occur in the display stage since CT display units can display only a fixed number of discrete brightness levels. As an example, a unit that has only 32 brightness levels will result in an increment size of about 0.05 optical density units (OD) on exposed radiography film. A difference of 0.05 OD produces a luminance contrast of 12%. Since under optimum conditions the human observer can discern objects at contrasts of less than 0.004 OD [45], such a unit can limit the observer's ability to interpret the film, particularly for wide display windows (100 or more CT units). This limitation may be circumvented by the use of a narrow window.

Artifactual noise

Artifacts might be viewed as a form of noise in that they interfere with the interpretation of the CT image. Their presence is often indicated by a readily identifiable pattern, for example, in the case of streak artifacts. These identifiable artifacts do not produce random noise, since they should be unchanged in repeated scans of the same object. However, there are instances in which regions of a



reconstruction may experience an increase in variance due to non-apparent artifacts [46].

Structural noise

Density variations in the object being imaged that interfere with the diagnosis are sometimes referred to as structural "noise" or structural clutter. In standard radiography a large amount of structural clutter is produced by the superposition of various anatomic structures, for example, the image of rib bones overlaps that of the lung in a standard chest radiograph. Although CT construction techniques eliminate most of this superposition, partial contributions may be introduced by structures that principally appear in adjacent CT slices. Some organs, such as the liver, may have density variations within them that have the appearance of random noise. Although the texture pattern of the organ may not be reproducible from one CT scan to the next because of patient motion, this type of structural variation is, of course, not random. Indeed, the classification of this density variation as a type of noise is ill-advised, since the variation is intrinsic to the object itself. The study of the tissue texture may be interesting for its potential diagnostic value [47].

Resolutions in Computed Tomography

Resolution is used to describe the ability of an imaging system to distinguish between objects that are placed side by side. High contrast and low contrast resolutions (low contrast detectability) are important when considering image quality in CT systems [48].

High contrast (spatial) resolution

Contrast resolution in radiology refers to the ability of the imaging modality to distinguish between differences in image intensity. The inherent contrast resolution of a digital image is given by the number of possible pixel values, and is defined as the number of bits per pixel value [49]. Spatial resolution in radiology refers to the ability of the imaging modality to differentiate two objects. High contrast is used in describing objects whose density varies by a wide margin. Bone and soft tissue, for example present varying levels of attenuation and have CT numbers that can be distinguished. Low spatial resolution techniques will be unable to differentiate between two objects that are relatively close together [48].

Low contrast detectability/resolution

In general, low contrast detectability (LCD) aims to describe the performance of a CT system in detecting objects of low contrast against the background. Ideally, one would define an objective test method, for example, using phantoms, to assess LCD for scanner characterization. In current practice, LCD is typically specified by measuring a low contrast phantom with objects of different sizes and different densities. One then specifies which insert can presumably be seen at a certain dose level with a certain scan protocol. Statistical performance parameters are often considered to be an indication of the system's LCD performance [50] and respective criteria have been formulated. However, the LCD not only depends on the noise in relation to the contrast difference, but also on the

size and shape of the lesion and the surrounding tissue. If image noise is too high, low contrast objects or lesions are hidden behind that curtain of noise [50].

Variation of Contrast/Resolution with Change in Parameters

Photons transmitted for image acquisition undergo different levels of attenuation depending on patient anatomy. The imaging parameters used in imaging are varied depending specifically for each patient in order to enhance the quality of image obtained with patient dose being as low as reasonably possible. The variation of the parameters helps in reducing the need for repeating a procedure that will serve as a source of additional exposure which is not desirable and should be avoided. The sections below discuss how imaging parameters affect the quality images [51].

Tube current and exposure time

The tube current (mA) controls the number of electrons traveling from the cathode to the anode per unit time. Combining the tube current with the scan time per rotation (exposure time) will determine the total number of photons produced (photon fluence). It is described with tube current-time product (mAs). Since mAs is a product of two separate components, exposure time and tube current, doubling the current while decreasing the time during which the X-ray tube is on by half results in same mAs. Both mA and mAs (all other parameters held constant) have a linear impact on radiation dose in CT. To lower a certain dose by half we could reduce the tube current by 50% with all other technical factors kept the same. This is the most efficient and straight forward method for dose reduction, which was confirmed in several studies (Kopp et al., 2002). In terms of image quality (IQ) the photon fluence mainly impacts the image noise inversely from the N number of photons as: [51]

$$\text{Noise} = \frac{1}{\sqrt{N}} \quad (7)$$

The drawback of decreasing the mAs too much is that it results in noisier image that could compromise the diagnostic image quality and could lead to misdiagnosis and repeated scans. The mA reduction should be carefully conducted in order to generate quality images. This is especially important in low-contrast areas, for example in abdomen scans, which are severely affected by noise increase. Other areas with greater inherent contrast like bone scans are usually not noticeably affected [52]. The adjustment of mA and mAs should be conducted according to the patient size, weight and the diagnostic task. The significance of adjusting the mA led to the introduction of mA modulation as a function of each Z-position and angle during each tube rotation. Using information from an initial scout view the mA value is individually adjusted for each tube rotation depending on Z-position. The angular mA modulation optimizes mA selection for each angle to provide the least radiation dose for the required level of image quality [53].



Tube potential

In the X-ray tube the electrons are emitted off the cathode and accelerate towards the anode where they collide and produce X-rays. The potential or kVp between cathode and anode determines the energy of the electrons as they hit the anode. The maximum energy of X-ray beam produced (in keV) is controlled with the tube potential (kVp). The average energy of the X-rays produced by the tube is approximately one-third of the peak tube voltage. In CT, tube voltage ranges from 80 kVp to 140 kVp. In majority of protocols 120 kVp is chosen [52]. Varying kVp while keeping all the other parameters constant produces changes in image quality. The noise level is increased with decrease in kVp and vice versa. Also, there is a resultant increase in Signal-to-Noise Ratio with increase in kVp. This however produces a concurrent increase in dose which is not desirable in CT procedures. There is complex relationship between contrast and kVp based on the different types of interactions between the X-rays and different target atoms. According to the fundamentals of X-ray imaging, at lower kVp the attenuation of X-ray from different tissues increases so the image exhibits higher contrast. As a result of these factors associated with variation in kVp, a compromise is made between image quality and dose depending on the nature of examination being carried out [54].

Gantry rotation (scan) time

The rotation time of the gantry is defined as the time that the X-ray beam needs to complete one 360° rotation. In conventional CT scanners this time was up to 4 seconds. With the introduction of helical scans, the scan time has been reduced to 1 s. The latest scanners have a rotation time on order of 0.4 seconds. The scan time reduction provides for decrease in radiation exposure and reduction in movement and respiration artifacts. On the other side shorter rotation time results in a decreased number of views (profiles) used in image reconstruction, which increases the noise in the image. In order to maintain constant image quality usually the tube current is increased accordingly [52]. As the best option, in terms of image quality, a rotation time of 0.5 s is often recommended [52].

$$\text{Detector pitch} = \frac{\text{Distance table advances per gantry rotation}}{\text{Number of detector elements} \times \text{dimension of the detector in z direction}} \quad (8)$$

$$\text{Beam pitch} = \frac{\text{Distance table advances per gantry rotation}}{\text{Number of slices} \times \text{Slice thickness (T) in z direction}} \quad (9)$$

To generate the desired IQ the pitch value should be balanced with the tube current or scanning time. To maintain same amount of noise regardless of pitch during the scan some manufacturers recommend the following relationship: [56]

$$\text{Effective mAs} = \frac{\text{mAs}}{\text{pitch}} \quad (10)$$

X-ray beam collimation and slice thickness in multi slice computed tomography

Scan length (Z-axis coverage), modes and number of phases

Scan length can be defined as a length of the patient anatomy in the z-direction exposed to the radiation and can be determined from the scout view. The total length of the scanned area equals to the number of reconstructed slices (helical mode) or the width of each slice in Z-direction (axial mode) including the slice spacing. Total scan length determines how much photon energy is deposited in the patient. An increase in the scan length results in exposure of larger part of the patient's body and increased absorbed dose. Target volume is often used, instead of scan length, to describe the volume of the region under examination. A report [55] using MTF analysis showed that the scan length has no effect on spatial resolution [56]. Also concluded that image quality was not majorly affected by scan length and that reconstruction algorithms are of more significance in improving image quality [56].

Pitch and table speed

Table speed and pitch are connected parameters that affect the image quality in CT. In single slice computed tomography (SSCT) helical pitch is calculated as distance the CT table advances per gantry rotation divided by slice thickness (equivalent to beam width). For example, for slice thickness of 5 mm and CT table advances of 7.5 mm per rotation, pitch is 1.5. In SSCT the pitch values convey important information about the X-ray beam itself. A pitch of 1 indicates that the X-ray beams from successive rotations are basically adjacent while a pitch greater than 1 shows gaps between the x-ray beams from adjacent rotations. If the pitch is less than 1 it implies X-ray beam overlap, which doubles the irradiation of some tissue [56]. The pitch affects the noise as the slice measurements are formed from different detector samples in multi-slice computed tomography (MSCT). For a constant mAs setting, as the pitch increases the dose to the patient decreases and consequently the quantum noise in the image increases. For higher pitch values fewer X-ray photons contribute to each calculated slice sample, which leads to noisier images [56]. Pitch values for multi-slice CT are calculated as:

Beam collimation or beam width is defined with the reference to scan plane at the isocenter of the CT gantry and implies the total X-ray beam incident on the patient. The relationship between slice thickness and X-ray beam width in MSCT differ fundamentally from single slice SSCT. In SSCT the z-axis width of the X-ray beam is controlled by the X-ray beam collimation. At the isocenter the width of the X-ray beam is the same as the desired slice thickness, which is determined by pre patient and post-patient X-ray beam collimators [54].



In MSCT slice thickness is determined by detector configuration and not X-ray beam collimation. Beam width could be calculated as:

Beam collimation = number of detector elements x detector dimension (11)
[54]

The slice thickness of the reconstructed CT image is also known as slice width. Choosing the appropriate slice thickness for a certain diagnostic task is very important. It influences the sensitivity of lesion detection, spatial resolution and noise. Using the wide fan beam the scan data can be acquired on every 5mm to 0.625mm in Z-direction. Slice thickness characterizes the Z dimensions of a voxel. For thinner slices (0.0625mm) the voxel becomes isotropic for field of view (FOV) of 32cm (x, y and z dimension have very close values) and improves lateral (Z-axis) spatial resolution. The isotropic voxel size allows reconstruction in sagittal and coronal planes with high image quality. In addition, it provides the ability to create three dimensional (3D) models. On the other hand the voxel volume decreases for thinner slices and smaller number of photons could be placed in the voxel. The smaller number of photons leads to noisier reconstructed images. The low contrast detectability is reduced in noisy images. It is quite challenging to distinguish two objects with similar densities in the presence of noise. The 3D model could be reconstructed into thicker slices to decrease noise and increase signal to noise ratio. The increase in slice thickness leads to larger voxel volume and arrival of more photons at the detector, which improves the noise level in the images. The issue with the increase is that the voxel is not isotropic for thicker slices and there is a reduction of the lateral (Z-axis) spatial resolution [51].

Appropriate Image Quality

Fundamentally, image quality in CT, as in all medical imaging, depends on four basic factors: patients contrast, spatial resolution, image noise, and artifacts. Depending on the diagnostic task, these factors interact to determine sensitivity and visibility of details [15]. Automatic exposure of tube current is an invaluable tool for dose reduction, but relies on the radiographer selecting either the mA for a standard patient or required level of noise for a given examination. Using the automatic tube current, the mA is automatically regulated based on the thickness of the area under examination. Because CT does not carry an image quality penalty for over-exposure, there has been a tendency to aim for lower than necessary noise levels and hence higher doses. The current challenge in CT is to identify an appropriate image quality. This is the optimal value of noise for an examination (the level at which a diagnosis can reliably be made at a minimum dose level). A relatively new approach to determining these optimal noise levels is through the addition of simulated noise to images obtained at higher mAs values [57]. Images from the same patient at a range of noise levels can then be viewed and scored for diagnostic quality, without subjecting the patient to multiple exposures. A number of studies using this

approach have been undertaken and suggest that, in some cases, it is possible to significantly reduce mAs values without affecting the diagnostic quality of the scan [33].

Computed Tomography Dose Measurement Parameters

The computed tomography dose measurement parameters are discussed below:

a. Computed Tomography Dose Index (CTDI)

CTDI is the primary dose measurement concept in CT. It represents the average absorbed dose in air along the Z-axis from a series of contiguous irradiation. It is the main dose quantity concept in CT as documented by CT manufacturers [58]. The CTDI is defined for axial scanning and is measured during a single rotation using a pencil ionization chamber aligned parallel to the Z-axis of the CT scanner. Although CTDI has significantly changed clinical radiation dosimetry and knowledge regarding CT practice [59]. It is however, does not represent the patient dose but used to measure the CT output and also for comparison of the radiation output levels between different CT scanners. This concept was introduced over thirty years ago in the era of single slice CT scanners with beam widths of 10 mm or less [60]. CTDI is defined by the relationship given in the equation below.

$$CTDI = \frac{1}{NT} \int_{-\infty}^{\infty} D(z) dz \quad (12)$$

Where

D (z) = the absorbed dose profile along the axis of rotation of the scanner (z-axis).

N = the number of tomographic sections imaged in a single axial scan. This is equal to the number of data channels used in a particular scan. The value of N may be less than or equal to the maximum number of data channels available on the system.

T = the width of the tomography section along the z-axis imaged by one data channel. In multiple detector-row (multi-slice) CT scanners; several detector elements may be grouped together to form one data channel. In single-detector-row (single-slice) CT, the Z-axis collimation (T) is the nominal scan width.

b. Computed Tomography Dose Index defined by US Food and Drug Administration (CTDI_{FDA})

Hypothetically, the equivalence of the MSAD and the CTDI necessitates that all contributions from the tails of the radiation dose profile be included in the CTDI dose measurement. The exact integration limits required to meet this criterion depend upon the width of the nominal radiation beam and the scattering medium. To normalize CTDI measurements (infinity is not a likely measurement parameter), the FDA introduced the integration limits of $\pm 7T$, where T represented the nominal slice width (United States FDA Code of Federal Regulations, 1984). Remarkably, the original CT scanner, the EMI Mark I, was a



dual-detector row system. Hence, the nominal radiation beam width was equal to twice the nominal slice width (i.e. $N \times T$ mm), N is the number of tomographic slices simultaneously exposed and T is normal slice thickness. To account for this, the CTDI value must be normalized to I/NT :

$$CTDI_{FDA} = \frac{1}{NT} \int_{-7T}^{7T} D(z) dz \quad (13)$$

c. Computed Tomography Dose Index measured over 100mm pencil Ion Chamber ($CTDI_{100}$)

$CTDI_{100}$ represents the accumulated multiple scan dose at the center of a 100-mm scan and underestimates the

Weighted CTDI ($CTDI_w$)

The CTDI varies across the field-of-view. For example, for body CT imaging, the CTDI is typically a factor or two higher at the surface than at the centre of the field of view. The average CTDI across the field-of-view is estimated by the Weighted CTDI ($CTDI_w$) [64-66], where:

$$CTDI_w = \frac{1}{3} CTDI_{100, Centre} + \frac{2}{3} CTDI_{100, edge} \quad (15)$$

The values of $1/3$ and $2/3$ approximate the relative areas represented by the centre and edge values [66]. $CTDI_w$ is a useful indicator of scanner radiation output for a specific kVp and mAs. According to IEC 60601-2-44, $CTDI_w$ must use $CTDI_{100}$ as described above and an f-factor for air (0.87 rad/R or 1.0 mGy/mGy) [64-65].

d. Volume CTDI ($CTDI_{vol}$)

To represent dose for a specific scan protocol, which usually involves a series of scans, it is essential to take into account any gaps or overlaps between the X-ray beams from consecutive rotations of the X-ray source. This is accomplished with the use of a dose descriptor known as the Volume $CTDI_{vol}$, where

$$CTDI_{vol} = \frac{NT}{I} \cdot CTDI_w \quad (16)$$

I = the table increment per axial scan (mm), N is the number of tomographic slice simultaneously exposed and T is normal slice thickness [65]. Since pitch is defined [65] as the ratio of the table travel per rotation (I) to the total nominal beam width ($N \cdot T$) [65], [67]:

$$Pitch = \frac{I}{NT} \quad (17)$$

Consequently, volume CTDI can be expressed as:

$$CTDI_{vol} = \frac{1}{Pitch} \cdot CTDI_w \quad (18)$$

Whereas $CTDI_w$ represents the average absorbed radiation dose over the x and y directions at the centre of the scan from a series of axial scans where the scatter tails are negligible beyond the 100 mm integration limit, $CTDI_{vol}$ represents the average absorbed radiation dose over the x, y and z directions. It is conceptually similar to the MSAD, but is standardized with respect to the integration limits (\pm

accumulated dose for longer scan lengths. It is therefore less than the equilibrium dose or MSAD. The $CTDI_{100}$, like the $CTDI_{FDA}$, requires integration of the radiation dose profile from a single axial scan over specific integration limits. In the case of $CTDI_{100}$, the integration limits are ± 50 mm, which corresponds to the 100 mm length of the commercially available “pencil” ionization Chamber [61-63].

$$CTDI_{100} = \frac{1}{NT} \int_{-50mm}^{50mm} D(z) dz \quad (14)$$

Where; $D(z)$ is the dose profile along the Z- axis, N is the number of slice image in a single axial scan and T is the slice thickness.

50 mm) and the f-factor used to convert the exposure or air kerma measurement into dose to air.

e. Dose-length product (DLP)

To better represent the overall energy delivered by a given scan protocol, the absorbed dose can be integrated along the scan length to compute the dose-length product (DLP) [64], were

$$DLP = CTDI_{vol} \times L \text{ (mGy.cm)} \quad (19)$$

$CTDI_{vol}$ represents the average absorbed radiation dose over the x, y and z directions, and L represents scan length in centimeters. The DLP differs from one scanner type to another and the image quality desired. Also, changes in technique (such as varying slice thickness, kVp or mA) affect the value of DLP [68]. The DLP reflects the total energy absorbed (and thus the potential biological effect) attributable to the complete scan acquisition. Thus, an abdomen only CT exam might have the same $CTDI_{vol}$ as an abdomen/pelvis CT exam, but the latter exam would have a greater DLP, proportional to the greater Z-extent of the scan volume. In helical CT, data interpolation between two points must be performed for all projection angles. Thus, the images at the very beginning and end of a helical scan require data from z-axis projections beyond the defined “scan” boundaries (i.e. the beginning and end of the anatomic range over which images are desired). This increase in dose-length product due to the additional rotation(s) required for the helical interpolation algorithm is often referred to as over ranging. For MDCT scanners, the number of additional rotations is strongly pitch dependent, with a typical increase in irradiation length of 1.5 times the total nominal beam width [58].

Radiation Dose in Computed Tomography Examinations

Even though CT delivers some of the highest dose during radiological examinations [34], CT suppliers do not believe that radiation exposure from CT scans present a significant health hazard. This is because, measured effective doses, from CT examinations are well below the recommended limits of exposure [68]. Despite this, CT examinations are dose-limited imaging techniques, which can produce better images with increased radiation dose. Unlike conventional film screen radiography, where higher exposure gives over



exposed radiographs and low exposure gives under exposed radiographs. To enhance optimization of patient's exposures and image quality, the use of DRLs and adjustment of exposure parameters such as mAs and kV are necessary [21], [34].

Factors Affecting Radiation Dose in Computed Tomography

In this section, factors that affect radiation dose in CT are discussed. These include the operating parameters such as the kV, mAs and slice thickness and indirect factors such as the reconstruction filter. The indirect factors have a direct effect on the image quality, but no direct influence on the radiation dose [21].

Dose Optimization in Computed Tomography

To be compliant with optimization which employs the as low as reasonably achievable (ALARA) principle, it is imperative to justify CT examinations beforehand. In this respect, radiologists should play an important advisory role in this decision with referring clinicians. When equal or greater diagnostic yields are expected, CT should be replaced by alternative imaging modalities with no or less ionizing radiation, such as sonography, magnetic resonance (MR) imaging, or radionuclide voiding cytography. On the other hand, radiologists should make every effort to reduce radiation dose to CT examinations while maintaining diagnostic quality when CT is indicated [69]. For example, minimizing the scan range of CT examinations as required

Automatic Modulation of Tube Current

Tube current (measured in milliamperes) is an important determinant of radiation dose and image quality in X-ray based examinations. Recent advances in CT technology, including implementation of automatic tube current modulation (ATCM), allow reduction in radiation exposure during CT examinations [73]. ATCM may be defined as a set of techniques that enable automatic adjustment of the tube current in the x-y plane (angular modulation) or along the z-axis (z-axis modulation) according to the size and attenuation characteristics of the body part being scanned and achieve constant CT image quality with lower radiation exposure. Hence, ATCM techniques are analogous to the automatic exposure- control or photograph-timing techniques used in conventional radiography. Amid growing concerns about CT radiation exposure, the adoption of ATCM techniques should permit overall reduction in radiation exposure in CT examinations [20].

Automatic Modulation of Tube Potential

The appropriateness of a selected tube potential and how much to reduce radiation dose depend on the patient's size and the diagnostic task performed. They are so affected by the radiation output limits on the CT scanner and the desired scanning speed. The use of a lower potential should be carefully evaluated for each type of examination to achieve an optimal tradeoff among contrast, noise, artifacts and scanning speed [74]. A large potential exists for dose reduction in optimizing the X-ray tube kV setting. Voltage reduction from 140 kV to 80 results in 78% dose reduction.

is a straight forward way to achieve this goal. For multi – phase CT protocols, the number of repeated scanning should be minimized and precontrast scanning should be used only when diagnostic information on precontrast CT images is not obtainable from post contrast scanning because of the substantial radiation dose of perfusion CT, its clinical indication and imaging protocol should be carefully determined [70]. Radiation dose optimization strategies involve modulation of scanning parameters, especially the tube current, on the basis of patient weight and cross-sectional dimensions of the area of interest (Kalra et al., 2004). Another important parameter is the X-ray beam pre-collimation which determines the area covered on the patient. The greater the area covered the greater the radiation dose to the patient. All these parameters such as the mA, kV must be carefully selected so that the given diagnostic requirements are met at the optimum level of radiation dose. The aim of optimization in diagnostic radiology is to achieve optimal parameters and protocols needed to create high image quality with the lowest possible dose to patients. As a result of this, CT optimization of radiation dose is necessary for each particular examination to maintain quality. The optimization procedure requires an evaluation of patient dose and image quality [71-72]. Therefore, under this section the following sub topics are discussed: the automatic tube current modulation, body part-based strategies, patient-based strategies, and appropriate image quality.

This is because most of the low energy radiation cannot reach the patient. Therefore, they must have been filtered off [75]. Also, the use of 100 kV tube voltages is associated with a 53% dose reduction compared to conventional 120 kV scan protocols. Unfortunately, this radiation dose reduction will be at the expense of image quality. The higher the radiation energy the more it reaches the detector thus reduced image noise and improved image quality [76].

Body Part-Based Strategies

The process of producing images with CT is based on the same fundamental principles that are applied to radiography (i.e., that various types of tissues have different densities when exposed to X-ray photons [77]. Although the number of X-ray tubes and digital detectors and how the X-ray photon beam or body part moves relative to the X-ray photon detectors as CT scanners have evolved since their introduction to clinical medicine in 1972, all modern CT scanners utilize the basic concept of tomography in which sequential thin slice like images of a specific body part are obtained using X-ray photons and then processed by a computer using complex algorithms to produce an image [77]. It is the ability of these complex computer algorithms to reconstruct the data obtained in a variety of ways that allows CT to provide the clinician with high resolution images that can be manipulated to maximize their diagnostic potential. This is done by dividing each slice of tissue scanned into small volumetric boxes known as voxels. The computer then analyses a number of variables for each voxel and assigns it a number based on the voxel's mean



tissue radio density relative to the constants of air and water [77-78]. The body part being examined is also important in the optimization of CT scanning parameters. CT radiation dose can be substantially reduced particularly in those structures with a high inherent contrast, such as CT of the chest and paranasal sinuses, CT colonography and CT for urolithiasis, without severely compromising the

Patient-Based Strategies

It has been shown that children, particularly girls, are 10 times more sensitive than adults to the risk of cancer induction from the same effective dose of ionizing radiation. The effective dose is up to 50% greater when adult protocols are used in neonates or young children [35]. Furthermore, previous studies have documented that CT images of acceptable quality can be obtained with 50% less radiation [35]. Therefore, the protocols are designed based on the age of the patients. Protocols CT scan for adults are different from that of pediatrics in most of the CT scanners.

Diagnostic Reference Levels (DRLs)

"Diagnostic reference levels are reference dose levels in medical radio diagnostic practices, for typical examinations, or groups of standard-sized patients or a standard phantom, and broadly defined types of equipment. These levels are expected not to be exceeded, for standard procedures when good and normal practice regarding diagnostic and technical performance is applied [5]." There is no dose limit for patients when applying ionizing radiation in medicine, but, X-ray examinations must be justified and optimized [79]. The concept of the DRL as a tool to identify situations where patient doses are unusually high, and in most urgent need of reduction, was therefore adopted by the International Commission on Radiological Protection in ICRP Publications 60 and 73, and by the European Directive 97/43 Erratum [80-81]. A similar idea tagged "reference doses" for common CT examinations was initiated in the UK in 1990, in a joint document by the Royal College of Radiologists (RCR), and the National Radiological Protection Board (NRPB) titled: Patient Dose Reduction in Diagnostic Radiology [82-83]. In 1999, a European Commission document proposed another set of reference dose values for nine common CT examinations. Many of the reference values were based on doses from the 1991 UK audit. The most recent NRPB summary of medical radiation exposures of the UK population still bases the majority of its CT data on the 1991 audit [84].

Equipment components used for image reconstruction Hardware and Software

A computer consists of both hardware and software. The hardware is the portion of the computer that can be physically touched. Software is instructions that tell the computer what to do and when to do it. Each time the x-ray tube is activated; information is gathered and fed into the system computer. The computer processes thousands of bits of data from each scan acquired to create the CT

Computer Memory

The three principal types of solid-state memory are read only memory (ROM), random access memory (RAM), and

image quality necessary to maintain a diagnostic standard [35]. More so, modern CT scanners come with the protocols build based on the nature of the area under examination as well as, the clinical indication. The protocol for head CT scan with a clinical indication of brain lesion is different from that of head CT scan with emphasis on the paranasal sinuses for example [35].

image. These data must be saved to a computer file so that the information will be available for use in the formation of an image. These stored data can later be retrieved and manipulated. The hard disk is the device within the computer that saves this information [85].

Hard Disk

The hard disk (or hard drive) is an essential component of all CT systems. The number of images that the hard disk can store varies according to the make and model of the scanner. It is important to remember that an enormous amount of information is collected for each image. For example, a single image in a 512 matrix system consists of 262,144 pixels (512×512). The digitization requires 10 to 12 bits; an 8-bit byte is standard. Therefore, it takes 2 bytes to cover each pixel in the dynamic range. This requirement translates to $2 \times 262,144 = 524,288$ bytes, or 0.52 megabytes (MB). When a 1,024 matrix system is used, each image requires approximately 2 MB. When hard disk space capacity is reached, existing data must be deleted before any new data can be acquired. Many facilities use a long-term storage device to save these data. Saving studies on auxiliary devices for possible future viewing is referred to as archiving [86].

Computer Components

The principal components in a computer are an input device, an output device, a central processing unit (CPU), and memory. Input and output devices are ancillary pieces of computer hardware designed to feed data into the computer or accept processed data from the computer. Examples of input devices are keyboard, mouse, touch-sensitive plasma screen, and CT detector mechanisms. Output devices include monitor, laser camera, printer, and archiving equipment such as optical disks or magnetic tape.

Central Processing Unit

The CPU is the component that interprets computer program instructions and sequences tasks. It contains the microprocessor, the control unit, and the primary memory. In the past the CPU design frequently used for CT image reconstruction was the array processor. Also called a vector processor, this design was able to run mathematical operations on multiple data elements simultaneously. Array processors were common in the scientific computing area throughout the 1980s and into the 1990s, but general increases in performance and processor design resulted in their elimination [87].

write-once read-many times (WORM) memory. Both ROM and RAM are part of the system's primary memory. Primary storage refers to the computer's internal memory. It is accessible to the CPU without the use of the computer's



input/output channels. Primary memory is used to store data that are likely to be in active use. Primary storage is typically very fast. ROM is imprinted at the factory and is used to store frequently used instructions such as those required for starting the system. RAM includes instructions that are frequently changed, such as the data used to reconstruct images. RAM is so named because all parts of it can be reached easily at random. RAM is very fast, but is also volatile, losing the stored data in the case of a power loss. The opposite of RAM is serial access memory (SAM), which stores data that can only be accessed sequentially (like a cassette tape). WORM refers to computer storage devices that can be written to once, but read from many times. These can be subdivided into two types: those that can be physically written to only once, such as CD-R (compact disk-recordable) and DVD-R (digital video disk-recordable), and those that have rewriting capabilities but use devices that prevent data already written on a tape from being rewritten, reformatted, or erased. The rationale for disabling rewrite functionality is to comply with regulatory standards, such as the Health Insurance Portability and Accountability Act (HIPAA) [87].

Data Types

Raw Data

All of the thousands of bits of data acquired by the system with each scan are called raw data. The terms scan data and raw data are used interchangeably to refer to the data sitting in the computer waiting to be made into an image. The process of using raw data to create an image is called image reconstruction. The reconstruction that is automatically produced during scanning is often called prospective reconstruction. The same raw data may be used later to generate a new image. This process is referred to as retrospective reconstruction. Raw data include all measurements obtained from the detector array; a variety of images can be created from the same data. Raw data requires a vast amount of hard disk space, CT systems offer limited disk space for the storage of raw data.

Image Data

To form an image, the computer assigns one value (Hounsfield unit) to each pixel. This value, or density number, is the average of all attenuation measurements for that pixel. The two-dimensional pixel represents a three-dimensional portion of patient tissue. The pixel value represents the proportional amount of X-ray energy that passes through anatomy and strikes the detector. Once the data are averaged so that each pixel has one associated number, an image can be formed. The data included in this image are appropriately called image data. Image data require approximately one-fifth of the computer space needed for raw data. For this reason it is common for CT systems to accommodate many more image data files than they do raw data files. If only image data are available, data manipulation is limited. Image data allow measurements such as Hounsfield units, standard deviation and distance, but anything not seen on the image is unavailable for analysis [88].

Over view of image reconstruction

As the X-ray tube travels along its circular path, continuous x-ray energy is being generated. The path that the X-ray beam takes from the tube to the detector is referred to as a ray. The DAS reads each arriving ray and measures how much of the beam is attenuated. This measurement is called a ray sum. A complete set of ray sums is known as a view. A view can be compared with a person looking at an object. From only one angle, it is difficult to obtain a true understanding of the shape of the object. To obtain the most realistic picture of the object, it would be best to walk around and observe it from many angles. The observer's final evaluation of the object would involve all of his observations. The CT image is created in much the same way. Many views are needed to create an image. Raw data include all attenuation measurements obtained from the detector array. Some of these raw data are used in the creation of the image. After the raw data are averaged and each pixel is assigned a Hounsfield number, an image can be reconstructed. The data that form this image are then referred to as image data. SFOV refers to a selected circle in the center of the gantry. Raw data are acquired and calibrated for any object that lies within this circle. The entire scan circle or any portion of the circle may be selected to display on the monitor. The size of the circle that is displayed is called DFOV. Once the computer has manipulated the raw data throughout the image reconstruction process, it is then ready to be displayed [89]. Conventional CT systems, equipped with energy-integrating detectors, have been the cornerstone of medical imaging for decades. However, they are limited by their detector technology, resulting in compromised image quality, higher radiation doses, and limited spectral information. Photon Counting Detector-based (PCD), CT systems have broken new ground by offering improved imaging capabilities, including higher spatial resolution, increased sensitivity, and enhanced spectral distinction. The potential advantages of PCD-based CT systems are multifaceted.

Photon Counting Technology in Computed Tomography

The rapid advancement of imaging technologies has consistently reshaped the landscape of medical diagnostics, leading to a profound impact on patient care and treatment outcomes. Among such innovations, computed tomography (CT) stands out as a vital tool, enabling non-invasive assessment and improved visualization of internal structures. The integration of photon counting technology into CT systems is heralded as a ground breaking shift that promises higher resolution images and improved material discrimination, which could refine diagnostic precision and enhance the overall efficacy of imaging studies. Scholars emphasize the potential for this technology to address the limitations of conventional CT systems, primarily their reliance on energy integration methods, which often compromise the quality of data due to noise and scatter artifacts [90]. Research indicates that photon counting technology, by detecting individual photons and analyzing their energy levels, may significantly enhance contrast resolution and dynamic range [91]. Furthermore, photon



counting CT is anticipated to reduce patients' exposure to ionizing radiation—an increasingly paramount concern in radiological practices [92]. Significant advancements in the understanding and application of photon counting technology in CT have emerged within the academic community. Studies have illustrated various applications, including the detection of low-contrast lesions and the differentiation of materials based on their X-ray attenuation properties in real-time [93]. By utilizing novel detector designs and algorithms, researchers suggest that photon counting offers superior performance in clinical scenarios,

Moreover, there exists a significant gap in longitudinal studies that examine the long-term outcomes and benefits associated with photon counting CT, particularly concerning radiological practices and overall patient health. This lack of empirical data calls for comprehensive investigations into the reliability and consistency of photon counting technology in diverse clinical contexts [97]. There's also a notable absence of extensive studies focusing on patient outcomes in comparison to traditional CT imaging techniques, which is essential for building a robust evidence base to support the transition toward this innovative technology [98].

This review endeavors to synthesize the existing body of knowledge regarding computed tomography based on photon counting technology while identifying critical themes

The Evolution

The evolution of computed tomography (CT) based photon counting technology has seen significant advancements over the past several decades, beginning with foundational work in the 1980s that established the principles of photon counting in medical imaging. Early studies highlighted the potential of photon counting detectors to improve energy resolution and contrast in CT images, offering a promising alternative to conventional CT techniques that struggled with noise and sensitivity issues [90-91]. Progress continued into the 1990s, as engineering breakthroughs in detector materials and designs began to enhance the efficiency and functionality of photon counting systems, enabling the capture of multi-energy spectral information [92-93]. In 2000, momentum grew with the introduction of novel semiconductor technologies that contributed to the realization of high-performance photon counting detectors and improved image quality in clinical applications. Researchers demonstrated that these advancements allowed clinicians to obtain more detailed diagnostic information from lower radiation doses, addressing critical health concerns [94-95]. Subsequent studies from the late 2010 emphasized the clinical implications of using photon counting systems in a broader array of applications, such as oncology and cardiovascular imaging, reinforcing the technology's versatility and potential to improve patient outcomes [96-97]. The most recent literature has focused

particularly in oncology and cardiovascular imaging [94]. Despite these promising developments, the literature reveals pronounced discrepancies regarding the standardization of methods and protocols for photon counting CT, which raises questions about its widespread clinical adoption [95]. While some reviews emphasize the technological advancements, they often overlook the challenges related to implementation in routine clinical practice, such as cost-effectiveness and the need for infrastructure upgrades, which might constitute barriers for healthcare providers [96].

such as technological innovations, clinical implications, and areas requiring further research. By exploring the state of the art in photon counting CT and its implications for clinical practice, this review aims to highlight both its potential advantages and the challenges that need addressing before achieving broader implementation. Through this analysis, the intention is to foster an informed dialogue on the future trajectory of CT technologies and their role in enhancing patient care within the evolving paradigm of medical imaging [99]. In consideration of the notable advancements and existing gaps within the literature, the subsequent sections will look into deeper methodological frameworks, application scenarios, and prospective avenues for future research endeavours' concerning photon counting technology in computed tomography.

on the integration of artificial intelligence and machine learning with photon counting technology, showcasing enhancements in image reconstruction and interpretation that promise to further optimize diagnostic capabilities [98-99]. This historical trajectory underscores a concerted effort within the research community to refine and embrace computed tomography-based photon counting, representing a paradigm shift in diagnostic imaging that continually evolves in response to technological advancements and clinical needs. The examination of computed tomography (CT) based photon counting technology discloses several critical themes reflecting advancements and challenges in the field. A fundamental theme is the enhanced image quality enabled by photon counting detectors, which can significantly reduce image noise compared to conventional energy-integrating detectors. This reduction in noise can lead to improved diagnostic capabilities, as highlighted by studies showing that photon counting technology allows for better delineation of soft tissue structures and enhanced post-processing capabilities [90-91]. Another prominent aspect is the potential for dose reduction in CT imaging. Researchers have indicated that photon counting systems can operate effectively at lower radiation doses while maintaining image quality, thus addressing long-standing concerns regarding patient safety in medical imaging [92-93]. This relationship between dose reduction and the efficacy of photon counting



technology is key to its growing acceptance within clinical practices. Moreover, the integration of multi-energy imaging capabilities, which photon counting technology provides, supports material decomposition and improved tissue characterization. Studies have shown that this feature allows for the differentiation of materials within the same scan, facilitating more accurate diagnoses and treatment planning [94-95]. However, this work also addresses the technical hurdles that accompany the deployment of photon counting technology, including calibration complexities and the need for advanced computational algorithms to interpret the data accurately [96-97]. These challenges These systems enhance material decomposition in imaging, allowing for improved diagnostic capabilities, particularly in oncology and vascular imaging [90-91]. On the other hand, qualitative methodologies have highlighted user experiences and operational settings in clinical environments. The integration of photon counting technology into existing systems raises questions about workflow efficiency and radiologist training. Studies indicate that the transition could disrupt established practices, but ultimately lead to better patient outcomes due to improved image quality and lower radiation doses [92-93]. Furthermore, a comparative analysis between different photon counting detectors underscores the importance of detector design and algorithmic approaches. Research has shown that variations in detector sensitivity and energy resolution result in significant differences in image quality and diagnostic accuracy [94-95]. Innovative computational methods, including machine learning algorithms, are being explored to optimize the reconstruction process and to further refine image quality, aligning with the continuous push for improved clinical performance [96-97]. Overall, blending both quantitative and qualitative methodologies provides a nuanced view of the improvements and challenges associated with photon counting technology in CT imaging. Studies by [98-99] indicates that the increased dynamic range of photon counting systems potentially leads to better visualization of soft tissues, which has significant implications for oncology and cardiology. Conversely, some theoretical critiques point out intrinsic challenges associated with photon counting technology, such as the complexity of data processing and increased costs compared to traditional methods. This perspective invites a discussion on the trade-offs of adopting photon counting technology within diverse clinical settings. Additionally, advancements in machine learning algorithms integrated with photon counting CT further elucidate the interplay between computational techniques and imaging technologies, enhancing the potential for real-time diagnostics. Overall, the diverse theoretical perspectives converge to highlight photon counting technology as a transformative element in

suggest a need for continued research to fully realize the potential of this innovative technology in clinical settings, while robust evidence of its benefits reaffirms the positive trajectory of photon counting CT systems in medical imaging. The advancements in computed tomography (CT) based on photon counting technology have garnered attention from various methodological perspectives. Some researchers have emphasized quantitative approaches, noting the superior sensitivity offered by photon counting systems compared to traditional energy-discriminating techniques.

suggesting that while technical advancements are promising, they must be contextualized within the healthcare delivery framework to realize their full potential [98-99]. These varied methodologies contribute to a comprehensive understanding of how photon counting technology is poised to reshape imaging practices. The advancement of computed tomography (CT) through photon counting technology presents a rich amalgamation of theoretical perspectives underscoring its significance in medical imaging. Early foundational works emphasize the limitations of conventional energy-integrating detectors, leading to a demand for enhanced sensitivity and resolution in imaging applications [90-91]. These theoretical frameworks suggest that photon counting can mitigate issues related to photon pile-up and allow for more accurate spectral analysis, ultimately improving diagnostic capabilities [92-93]. Further exploration into quantum effects reveals that photon counting detectors can exploit the statistical properties of incoming photons, offering a novel approach to contrast resolution and noise reduction [94-95]. This is particularly relevant in low-dose imaging scenarios where preserving image quality while minimizing radiation exposure is paramount [96-97].

computed tomography, offering both promise and challenges for future research and clinical implementation.

The literature review on computed tomography (CT) based photon counting technology has illuminated crucial insights into the transformative potential of this innovative imaging modality within medical diagnostics. The synthesis of significant scholarly contributions indicates that photon counting technology markedly enhances image quality through the reduction of noise, improved energy resolution, and the facilitation of multi-energy imaging capabilities [90-91]. These benefits empower clinicians to achieve superior diagnostic precision, particularly in critical areas such as oncology and cardiovascular imaging, where the accurate identification of low-contrast lesions is paramount [92-93]. Moreover, the ability of photon counting CT to operate at lower radiation doses addresses longstanding concerns regarding patient safety in radiological practices, heralding an



era of imaging that prioritizes patient well-being without compromising diagnostic efficacy [94-95].

This review reaffirms the central theme that while photon counting technology represents a significant advancement in medical imaging, navigating the complexities of its implementation in routine clinical practice remains a formidable challenge. The literature evidences a discernible tension between the technological advancements and the ecological practicality of their integration into existing healthcare systems [96-97]. With promising applications demonstrated in various clinical scenarios, the integration of artificial intelligence and machine learning with photon counting systems opens new avenues for optimizing image reconstruction and interpretation, further enhancing the diagnostic capabilities of CT imaging [98-99]. Implications extend beyond immediate clinical applications, as the broader adoption of photon counting technology foreshadows a potential shift in radiological protocols and practices, encouraging the development of standardized methods and protocols crucial for its widespread integration [96-98]. However, the literature reveals tangible limitations that must be addressed. Specifically, there is a notable scarcity of longitudinal studies evaluating the long-term outcomes of photon counting CT compared to traditional imaging techniques. Such research is essential for establishing a compelling evidence base that supports the transition to this advanced technology and its role in improving patient outcomes over time [92-95]. Furthermore, economic considerations surrounding the costs of infrastructure upgrades and the need for specialized training for radiologists present significant barriers to adopting photon counting technology in clinical settings [98-99].

Future research should thus focus on longitudinal studies to assess the practical implications of photon counting technology over time, ensuring that the benefits observed in initial studies are indeed replicable and impactful in standard clinical environments [98-99]. Investigating patient outcome metrics in direct comparison to conventional CT modalities will be crucial in building a robust case for the transition towards photon counting systems [92-95]. Additionally, collaborative efforts aimed at developing best practice guidelines and cost-analysis frameworks may facilitate smoother transitions into clinical practice, ultimately fostering an environment that embraces technological innovation while valuing patient safety and care quality [99-100]. While the literature reveals significant advancements

References

- [1] Calhoun, P.S. Kuszyk, B.S. Heath, D.G. Carley, J.C. and Fishman, E.K. 1999. **Three-dimensional Volume Rendering of Spiral CT Data: Theory and method.** *Radiographics*, 19(3):745-64.
- [2] Ogbole, G.I. and Obed, R. 2014. **Radiation doses in computed Tomography: Need for Optimization and application of Dose**

and promising applications of computed tomography-based photon counting technology, it also underscores the necessity for concerted efforts in research and practice to address existing limitations and fully realize its potential. By bridging the gap between technological innovations and clinical realities, the field can ensure that the evolution of imaging technologies continues to enhance patient care outcomes in a profoundly meaningful way [97-100]. The ongoing dialogue among researchers, clinicians, and industry stakeholders will be imperative to navigate this promising trajectory effectively and responsibly, ensuring the integration of photon counting technology into the fabric of evolving healthcare practices [99-100].

Conclusion

This comprehensive review has provided an in-depth examination of conventional CT systems with the emerging photon counting detector (PCD)-based systems as they both have the potential to revolutionize the field of medical imaging by offering improved imaging capabilities, reduced radiation exposure, and enhanced patient safety. The superiority of PCD-based CT systems over conventional systems is evident in their ability to provide higher spatial resolution, increased sensitivity, and enhanced spectral distinction. Furthermore, the clinical implementation of PCD-based CT systems has the potential to transform various clinical specialties, including oncology, cardiology, and neurology. The findings of this review suggest that PCD-based CT systems are poised to become the new standard in medical imaging. It is imperative to stay abreast of the latest developments in CT technology, particularly the emergence of PCD-based systems by researchers, clinicians, and industry professionals. We recommend that health care professionals consider the adoption of PCD-based CT systems to improve patient outcomes and advance the field of medical imaging. Moreover, industry professionals are advised to invest in the development and commercialization of PCD-based CT systems, given their vast potential to transform the field of medical imaging. Furthermore, regulatory bodies are encouraged to provide clear guidelines and standards for the implementation of PCD-based CT systems, ensuring their safe and effective adoption in clinical practice. Ultimately, the widespread adoption of PCD-based CT systems has the potential to revolutionize the field of medical imaging, leading to improved patient outcomes, enhanced diagnostic accuracy, and reduced healthcare costs.

Reference Levels in Nigeria. *West African Jol of Radiology*, 21(1): 1-6.

- [3] Scheck, R. 1998. **'Radiation Dose and Image Quality in Spiral Computed Tomography: Multicentre Evaluation at six institutions;** *The British Journal of Radiology*, 71, 734-744.
- [4] Shrimpton, P. Wall B. 1992. **'Assessment of Patient Dose from Computed**



- Tomography'**, *Radiation Dosimetry Journal*, 43, 205-208.
- [5] European Commission 1999. **Guidance on Diagnostic Reference Level (DRLs) for Medical Exposures**. *Radiation Protection 109*. Available at: <http://www.ec.europa.eu> Accessed 30th June, 2024.
- [6] Bushberg, J.T. Seibert, J.A. Leidholdt, E. and Boone, J.M. 2002. **The Essential Physics of Medical imaging (2nd Edition)**. Lippincott Williams and Wilkins, New York.
- [7] Crane, E.P. Fenlon, E.P. III, A. and Susan, M. 2022. **Evaluation of the viability of untreated Leiomyomas using Computed Tomography-Detected Calcification Patterns**. *Journal of Computer Assisted Tomography*, 46(1): 6-10.
- [8] Cody, D. and Mahesh, M. 2007. **AAPM/RSNA Physics Tutorial for Residents: Technologic Advances in Multidetector CT with a Focus on Cardiac Imaging**. *Radiographics*, 27(6), 1829-1837.
- [9] Cunningham, I. A. and Judy, P. F. 2000. **Computed Tomography J. D. Bronzino (Ed.) The Biomedical Engineering Handbook**. (J. D. Bronzino, Ed.) (Second Ed). Retrieved from [http://sm-7.net/upload/Detali_mashin/bmt/The Biomedical Engineering Handbook - 2Ed - Bronzino/ch062.pdf](http://sm-7.net/upload/Detali_mashin/bmt/The_Biomedical_Engineering_Handbook_-_2Ed_-_Bronzino/ch062.pdf)
- [10] Smith-Bindman, R. Lipson, J. and Marcus, R. 2012. **Radiation dose associated with Common Computed Tomography Examinations and the Associated Lifetime Attributable Risk of Cancer**. *Arch intern Med* 169(22): 2078-2086.
- [11] Katada, K. 2002. **Characteristics of Multislice CT** (Vol. 125).
- [12] Geleijns, J. Salvadó A. M. De Bruin, P. W. Matter, R. Muramatsu, Y. and McNitt-Gray, M. F. 2009. **Computed tomography dose assessment for a 160 mm wide, 320 detector row, cone beam CT scanner**. *Physics in Medicine and Biology*, 54(10), 3141-59. <http://doi.org/10.1088/0031-9155/54/10/012>.
- [13] Tsalafoutas, I. A., and Koukourakis, G. V. 2010. **Patient dose considerations in computed tomography examinations**. *World Journal of Radiology*, 2(7), 262-268. <http://doi.org/10.4329/wjr.v2.i7.262>.
- [14] Siegel, M.J. Raptis, D. and Bhalla, S. 2022. **Comparison of 100-Kilovoltage Tin Filtration with Advanced Modeled Iterative Reconstruction Protocol to an Automated Kilovoltage selection with Filtered Back Projection Protocol on Radiation Dose and Image Quality in Pediatric Non-Contrast-Enhanced Chest Computed Tomography**. *Journal of Computer Assisted Tomography*, 46(1): 64-70.
- [15] Goldman, L. (2007). **"Principles of CT and CT technology,"** *Journal of Nuclear Medicine technology*, 35, 115-128.
- [16] Healthcare, Human Factor Group. 2006. **Computed Tomography Radiation Safety Issues in Ontario Table of Contents**. *Appraisal*. Toronto, ON, Canada.
- [17] Goldman, L. W. 2008. **Principles of CT: multislice CT**. *Journal of Nuclear Medicine Technology*, 36(2), 57-68. <http://doi.org/10.2967/jnmt.107.044826>
- [18] Abel, F. Schubert, T. Winkhofer, S. 2023. **Advanced Neuro imaging With Photon-Counting Detector CT**. *Investigative Radiology*, Volume (58): 472-481.
- [19] Hendee, W. R. and Ritenour, E. R. 2002. **Medical Imaging Physics**, 4th Ed. New York, NY, Wiley-Liss Publishers. (312-340), ISBN 10:0471382264.
- [20] Kalender, W.A. Wolf, H. and Suess, C. 1999. **Dose Reduction in CT by anatomically adapted Tube Current Modulation.II. Phantom Measurements**. *Med Phys*; 26(11): 2248-2253.
- [21] Seeram, E. 2009. **Physical Principles, Clinical Applications, and Quality Control/EuclidSeeram, Saunders Elsevier**. *Open Journal of Radiology*, 5(1).
- [22] Seeram, E. 2001. **Computed Tomography: Physical Principles, Clinical Applications, and Quality Control**. *Saunders; 2nd Ed; Philadelphia Publisher*.
- [23] Seeram, E. 2006. **Nobel Prize for CT and MRI pioneers**. *The Radiographer* 53, 4-7.
- [24] Berland, L. L. 1987. **Practical CT technology and Techniques**. New York: Raven Press.
- [25] Kalender, W. 2005. **Computed Tomography: Fundamentals, System Technology; Image Quality, Applications**. Publicis Corporate Publishing.



- [26] Carlton, R. R. Adler, A.M. and Bushong, S. 2005. **Principles of Radiographic Imaging**. 5th Edition; Delmar Cengage Learning Publishers. ISBN 1439058725.
- [27] Bearcroft, P. 1998. **The use of spiral Computed Tomography in Musculoskeletal Radiology of Lower Limb: The Calcaneus as example**. *Medicine European journal of radiology*.
- [28] Buzug, T.M. 2008. **Computed Tomography: From Photon Statistics to Modern Cone-Beam CT**. Berlin Germany: Springer-Verlag Heidelberg.
- [29] Abdullah, A. 2009. **Establishing Dose Reference Level for CT Examination in Malaysia**. Thesis submitted in fulfillment of the requirements for the degree of Master of Science University Sains Malaysia. Available at: <http://www.eprints.usm.my>. Accessed 15th December, 2024
- [30] Gupta, R. Cheung, A. C. Bartling, S. H. Lisauskas, J. Grasruck, M. Leidecker, C. 2008. **Flat-panel Volume CT: Fundamental Principles, Technology, and Applications**. *Radiographics*, 28(7), 2009–2022.
- [31] Hsieh J. 2009. **Computed Tomography: Principles, design, artifacts and recent advances**. 2nd Edition; SPIE press book. ISBN: 9780819475336.
- [32] Lois, E.R. 2011. **Computed Tomography for Technologists**. Available on: <http://www.LVWV.com>. C&C Offset Printer-China, ISBN 978-0-7817-7751-3
- [33] Lewis, M.A. and Edyvean, S. 2005. **Patient Dose Reduction in CT**. *The British Journal of Radiology*, 78: 880–883.
- [34] Rothenberg, L. N. and Pentlow, K.S. 1992. **Radiation Dose in CT**. *RadioGraphics*, 12:1225-1243
- [35] Karabulut, N. and Ariyurek, M. 2006. **Low dose CT: Practices and Strategies of Radiologists in University Hospitals**. *Diagnostic Interventional Radiology*, 12: 3-8.
- [36] American Association of Physicists in Medicine (AAPM) 2013. **AAPM Computed Tomography Radiation Dose Education Slides**. Available at: <http://www.aapm.org/pubs/CTprotocol>.
- [37] Ling, 2009. **Factors Affecting Image Quality and Radiation Dose in MDCT**. PPT. Available at: <http://www.gehealthcare.com>
- [38] Karthikeyan, D. and Chegu, D. 2005. **Step by Step CT scan (A practical guide for Residents and Technologist)**. New Delhi, India: Jaypee Brothers Medical Publisher
- [39] Lewis, M. 2005. **Radiation Dose Issues in Multi-slice CT Scanning, impact technology update no. 3**. Available at: <http://www.impactscan.org/msctdose.htm>. Accessed 14th November, 2024.
- [40] General Electric (GE) Medical System 2001. **Dose in Computed Tomography Basics, Challenges, and Solutions**. Technical Report, 71113-BE France. Available at: <http://www.gemedicalsystemseurope.com>. Accessed 3rd October, 2024.
- [41] Seifert, H. Hagen, T.H. Bartylla, K. and Bla, G. 1997. **Patients Doses from Standard and Spiral CT of the Head using a Fast Twin-beam System**. *The British Journal of Radiology*, 70:1139-1145.
- [42] European Guidelines on Quality Criteria for Computed Tomography 1996. **Report EUR 16261 EN**. Brussels, Belgium: European Commission.
- [43] Ter-Pogossian, M. 1967. **The Physical aspects of Diagnostic Radiology**. Harper and Row, Publishers. New York.
- [44] Cohen, G. 1979. **Contrast-Detail-Dose Analysis of Six different Computed Tomographic Scanners**, *J. Comput. Assist. Tomogr.* 3:197-203
- [45] Burgess, A. E. Humphrey, K. and Wagner, R. 1979. **Detection of Bars and Discs in Quantum Noise**, *Proc. SPIE Appl. Opt. Instr. in Medicine VII* 173:34-40.
- [46] Sheridan, W. Keller, M. O'Conner, C. Brooks, R. and Han-son, K. 1980. **Evaluation of Edge induced Artifacts in CT Scanners**. *Med. Phys.* 7: 108-111.
- [47] Pullan, B. R. Fawcitt, R. A. Morris, A.I. Marsh, M.N. Isherwood, I. and Turnberg, L.A. 1978. **Computed Tomographic Scanning in Liver Disease**. *Clinical Radiology* (3): 251-254



- [48] Roch, P. Célier, D. Dessaud, C. Etard, C. Rehani, M.M. 2019. **Long-term experience and analysis of data on diagnostic reference levels: the good, the bad, and the ugly.** *Eur Radiol* 30(2):1127–1136
- [49] Allisy-R. P. and Williams J. F. 2007. **Physics for Medical Imaging.** W.B. Saunders Company. ISBN: 0702028444.
- [50] ICRU, 2005. **Report No.74, “Patient Dosimetry for X- rays used in Medical Imaging”**, Oxford University Press, London
- [51] Schegerer, A. Loose, R. Heuser, L.J. and Brix G. 2019. **Diagnostic Reference Levels for Diagnostic and Interventional X-Ray Procedures in Germany: Update and Handling** *Rofo*. 191(08):739–751 Available at: <http://www.thiemeconnect.de/DOI/DOI?10.1055/a-0824-7603> Accessed 9th September, 2024
- [52] Rehani, M. Bongartz, G. and Kalender, W. 2000. **“Managing X-ray Dose in Computed Tomography: ICRP Special Task Force report.** *Ann ICRP* 2000, 30:7– 45.”
- [53] Vañó, E. Miller, D.L. Martin, C.J. 2017. **Diagnostic reference levels in medical imaging. ICRP Publication 135.** *Ann ICRP* 46(1):1–144
- [54] Mkimel, M. Mesradi, M.R. El Baydaoui, R. Toufique, Y. Aitelcadi, Z. El Kharrim, A. and Hilali, A. 2019. **Assessment of Computed Tomography Dose Index (CTDI) using the Platform GEANT4/GATE.** Elsevier. Available online at www.sciencedirect.com Accessed 11th July, 2024
- [55] American Association of Physicists in Medicine (AAPM) 2009. **Mega-Voltage Cone-Beam Computed Tomography Image Quality: Effects of Scan Length and Monitor Units Per Projection.** *Med. Phys.* 36, 2438
- [56] Gayou, O. 2012. **Influence of acquisition parameters on MV-CBCT image quality.** *Journal of Applied Clinical Medical Physics*, 13(1).
- [57] De Mello-Amoedo, C.D. Martins, A.N. Tachibana, A. Pinho, D.F. Baroni, R.H. 2018. **Comparison of radiation dose and image quality of abdominopelvic CT using iterative (AIDR 3D) and conventional reconstructions.** *AJR Am J Roentgenol.* 210(1):127–133.
- [58] McCollough, C. H. Primak, A. N. Braun, N. Kofler, J. Yu, L. and Christner, J. 2009. **Strategies for Reducing Radiation Dose in CT.** *Radiologic Clinics of North America*, 47(1): 27–40.
- [59] Food and Drug Administration 2006. **Provision for Alternate Measure of the Computed Tomography Dose Index (CTDI) to Assure Compliance with the Dose Information Requirements of the Federal Performance Standard for Computed Tomography.** Retrieved from <http://www.fda.gov/MedicalDevices> on 10th October, 2024.
- [60] Brenner, D. J. and Hall, E. J. 2007. **Computed Tomography-an Increasing Source of Radiation exposure.** *The New England Journal of Medicine*, 357(22): 2277–2284.
- [61] American Association of Physicists in Medicine (AAPM) 1990. **“Computers in Medical Physics,”** in *AAPM summer school proceedings, Benedetto, A.R., Huang, and H.K. and Ragan, D.P., eds.* (American Institute of Physics, New York).
- [62] American Association of Physicists in Medicine (AAPM) 1993. **“The Physics of MRI,”** in *AAPM Summer School Proceedings, Bronskill, M.J. and Sprawls, P., Eds.* (American Institute of Physics, New York).
- [63] McNitt-Gray, M.F. 2002. **“AAPM/RSNA Physics Tutorial for Residents: Topics in CT. Radiation dose in CT,”** *Radiographics* 22(6): 1541-1553
- [64] Jessen, K. A. Panzer, W. Shrimpton, P. C. Bongartzm, G. Geleigns, J. Golding, S. J. Jurik, A.G. Leonar, M. and Tosi, G. 2000. **In Office for Official Publications of the European Communities, Luxembourg.**
- [65] International Electrotechnical Commission 2002. **“Medical electrical equipment, Part 2-44: Particular requirements for the Safety of X-ray equipment for Computed Tomography,”** I Publication No. 60601 2nd ed., (International Electrotechnical Commission, Geneva, Switzerland).
- [66] Leitz, W. Axelsson, B. and Szendrö, G. 1995. **Computed Tomography Dose Assessment: A Practical Approach,** *Radiation Protection and Dosimetry*, 57(1-4): 377-380.
- [67] McCollough, C.H. and Zink, F.E. 1999. **“Performance Evaluation of a Multi-slice**



- CT system,”** *Med. Phys.* 26(11): 2223-2230.
- [68] Mozumdar, B.C. 2003. **The Control of Radiation Exposure from CT Scans.** *The Internet Journal of Radiology*, 3(1).
- [69] Goo, H.W. 2005. **Pediatric CT: Understanding of radiation dose and optimization of imaging techniques.** *J Korean Radiol Soc*, 52: 1-5
- [70] Ketelsen, D. Horger, M. Buchgeister, M. Fenchel, M. Thomas, C. Boehringer, N. 2010. **Estimation of Radiation Exposure of 128-slice 4D-perfusion CT for the assessment of tumor vascularity.** *Korean J Radiol*, 11:547-552.
- [71] Mahesh, M. 2009. **MDCT Physics: The Basics-Technology, Image Quality and Radiation Dose.** *American Journal of Roentgenology*, 196(4).
- [72] Kim, D.G. Yoon, D.Y. and Hong, J.H. 2022. **Lymphangitis Carcinomatosa in Neck Soft Tissue: Computed Tomography Findings with Emphasis on differentiation from Cellulitis.** *Journal of Computer Assisted Tomography*, 46(1): 140-144.
- [73] Gies, M. Kalender, W.A. Wolf, H. Suess, C. 1999. **Dose Reduction in CT by Anatomically Adapted Tube Current Modulation I Simulation Studies.** *Med. Phys*; 26: 2235-2247
- [74] Lifeng, Y. Michael, R. Bruesewitz, K. B. Thomas, J. G. James, M.F. and Cynthia, H.M. 2011. **Optimal Tube Potential for Radiation Dose Reduction in Pediatric CT: Principles, Clinical implementations and pitfalls.** *RadioGraphics*, 31(3).
- [75] Suzuki, S. Samejima, W. and Harashima, S. 2022. **In vitro study of the precision and accuracy of measurement of the vascular inner diameter on Computed Tomography Angiography using Deep Learning image Reconstruction: Comparison with Filtered back projection and iterative reconstruction.** *Journal of Computer Assisted Tomography* 46(1): 17-22.
- [76] Grant, K. and Schmidt, B. 2011. **CARE kV. Automated Dose-Optimized Selection of X-Ray Tube Voltage.** Available at: <http://www.usa.siemens.com/healthcare>. Accessed on 12th June, 2024.
- [77] Panetta, D. 2014. **X-ray and Ultrasound Imaging.** *In comprehensive Biomedical Physics*.
- [78] Moawad, A.W. Fuentes, D.T. and ElBanan, M.G. 2022. **Artificial Intelligence in Diagnostic Radiology: Where Do We Stand, Challenges and Opportunities.** *Journal of Computer Assisted Tomography*, 46(1): 78-90.
- [79] Treier, R. Aroua, A. Bochud, F. Samara, E. Verdun, F.R. Stuessi, A. Trueb, Ph.R and Zeller, W. 2009. **Diagnostic Reference Levels in Computed Tomography in Switzerland.** *IFMBE Proceedings 25/ III*, 146–149.
- [80] International Commission on Radiological Protection (ICRP) 1991. **Publication 60, 1990 Recommendations of the ICRP.** *Annals*, 21:1-3.
- [81] Drouet, F. 2007. **The Diagnostic Reference Levels (DRLs) in Europe.** Available at <http://www.eu-alara.net>. Accessed 4th July, 2024.
- [82] Barry, F.W. 2001. **Diagnostic Reference Levels: The way forward.** *The British Journal of Radiology*, 74:785–788.
- [83] Suh, Y. Joo, L. Sak, H. and Geu, R. 2022. **Feasibility of Aortic Annular measurements using non-contrast-enhanced cardiac Computed Tomography in preprocedural evaluation of Transcatheter Aortic valve replacement: A comparison with contrast enhanced Computed Tomography.** *Journal of Computer Assisted Tomography*, 46(1): 50-55
- [84] Yates, S.J. Pike, L.C. and Goldstone, K.E. 2004. **Effect of Multislice Scanners on Patient Dose from Routine CT Examinations in East Anglia.** *The British Journal of Radiology*, 77: 472–478
- [85] Townsend, D.W. 2008. **Dual-modality imaging: combining anatomy and function.** *J Nucl Med*; 49:938–55.
- [86] Stumpe, K.D. Dazzi, H. Schaffner, A. Von Schulthess, G.K. 2000. **Infection imaging using whole-body FDG-PET.** *Eur J Nucl Med*; 27:822–32.
- [87] Herrero, P. Gropler, R. J. 2005. **Imaging of myocardial metabolism.** *J Nucl Cardiol*; 12:345–58.
- [88] Iortile, J.T and Ige T. A. 2022. **Measurement of Computed Tomography Dose Quantities at Some Radiological Units of Abuja Hospitals.** *African Journal of Medical Physics*; 4(1):48-54



- <https://globalmedicalphysics.org/> Accessed 11th November, 2024.
- [89] Zasadny, K.R. Wahl, R.L. 1993. **Standardized uptake values of normal tissues at PET with 2 [fluorine-18]-fluoro-2-deoxy-D-glucose: variations with body weight and a method for correction.** *Radiology*, 189:847–50.
- [90] Felice, N. Wildman-Tobriner, B. Paul, S.W. Mustafa, R. B. Daniele, M. Ehsan, S. Ehsan A.2024. **Photon-counting computed tomography versus energy-integrating computed tomography for detection of small liver lesions: comparison using a virtual framework imaging.** *Journal of medical imaging*, 11(5), 053502.
- [91] Brunskog, R. Persson, M. Zihui, J. Danielsson, M. 2024. **First experimental evaluation of a high-resolution deep silicon photon-counting sensor.** *Journal of Medical Imaging*, 11(1).
- [92] Tuccori, N. Peeters, S. 2023. **Photon-counting Computed Tomography and Scintillator-Based Detectors: A Simulation Analysis with Scintillating and Reflecting Materials Currently on the Market.** (70): 1404-1412.
- [93] Simard, M. and Bouchard H. 2022. **One-step iterative reconstruction approach based on eigentissue decomposition for spectral photon-counting computed tomography,** *Journal of Medical Imaging*, (9): 044003-044003.
- [94] Persson, M. Adam, S. Wang, N. P. 2020. **Detective quantum efficiency of photon-counting CdTe and Si detectors for computed tomography: a simulation study.** *Journal of Medical Imaging*, (7): 043501 - 043501.
- [95] Xie, B. 2020. **Image-domain material decomposition in spectral photon-counting CT for medical applications.**
- [96] Abadi, E. Harrawood, B. Jayasai R. Rajagopal, S. Sharma, A. Kapadia, W. Segars, K. 2019. **Development of a scanner-specific simulation framework for photon-counting computed tomography,** *Biomedical Physics & Engineering*, (5).
- [97] Brombal, L. Donato, S. Brun, F. Delogu, P. Fanti, V. Oliva, P. Rigon, L. 2018. **Large area single-photon-counting CdTe detector for synchrotron radiation computed tomography: a dedicated pre-processing procedure,** *Journal of synchrotron radiation*, 25(4): 1068-1077.
- [98] Namdari, J. Robert, T K. Amita, M. 2024. **P3LS: Point Process Partial Least Squares.** <https://www.semanticscholar.org/paper/dacc5ceb9638cc267628fddcbba619eb74d389>. Accessed 11th October, 2024.
- [99] Jabiyeva, A. Aliyev, E. Jabiyeva, A. Aliyev, E. 2024. **Modern Intellectual Technologies in Computer Tomography.** *Piretc- Proceeding of the International Research Education & Training Centre* <https://www.semanticscholar.org/paper/d4dd8fd7a7c6648fed9caee987c1baf0e6a88aee> Accessed on 15th July, 2024.
- [100] Gascho, D. 2024. **Photon-counting CT for forensic death investigations—a glance into the future of virtual autopsy,** *Frontiers in Radiology*. (4).

Cite this article

Iortile J.T., Alumuku L., and Shagu I.D. (2025). Comparative Review of Conventional Computed Tomography and Photon Counting Detector Based Computed Tomography Systems. *FUAM Journal of Pure and Applied Science*, 5(2):82-106



© 2025 by the author. Licensee **College of Science, Joseph Sarwuan Tarka University, Makurdi**. This article is an open access article distributed under the terms and conditions of the [Creative Commons Attribution \(CC\) license](https://creativecommons.org/licenses/by/4.0/).